INTERACTION OF SHALLOW-WATER WAVES AND BOTTOM TOPOGRAPHY

B. Boczar-Karakiewicz

INRS-Océanologie
Université du Québec
Rimouski (Québec)
Canada G5L 3A1

J.L. Bona

Department of Mathematics
Pennsylvania State University
215 McAllister Building
University Park, PA 16802

D.L. Cohen

Massachusetts Institute of Technology
Lincoln laboratory
Lexington, Massachusetts 02173-0073

Abstract

A system of equations is proposed for the dynamical interaction of progressive surface waves and bottom sediment in near-shore zones. This system is shown to model the formation of stable, bar-like structures that are familiar features of many coastal areas.

Introduction

In this paper, interest will be directed toward the description of surface waves in comparatively shallow water and their mutual interaction with the topography over which they propagate. Because the water is shallow, the fluid motions extend to the bottom and so the waves typically undergo a change of form as they progress. If the fluid lies over a bed of loose sediment, such as sand, then the passage of waves may in turn have an effect on the bottom. As the bed changes shape, the surface waves will deform differently. Thus the entire system in view, comprising both the fluid and the bed surfaces, admits the possibility of complex self-interactions.

A primary motivation of this study is the desire to understand the formation

of bars along the coasts of large bodies of water. We will accordingly concentrate on a two-dimensional situation wherein deep-water, plane, periodic wavetrains impinge on shallow-water zones. Field observations of situations that roughly correspond to this idealization have repeatedly identified quasi-static arrays of bars and troughs. In the more controlled environment of the laboratory wavetank, experiments have shown that periodic wavetrains incipient on an initially featureless bed of sand will eventually organize an equilibrium configuration of bars and troughs. An ocean coast may have incoming, deep-water waves with typical wavelengths of a hundred meters and sand bars spaced one-quarter to one-half a kilometer apart, whereas the scales that pertain in the laboratory may be a hundred times smaller. Despite the disparate scales, the laboratory and field phenomena of bar formation are strikingly similar, leading one to conjecture that such manifestations may depend upon some relatively simple and universal wave-bottom interaction. This optimistic view is quickly tempered by the variety that nature provides, and it must be candidly admitted that no single explanation is likely to cover all situations. Nevertheless, the ideas put forth below appear to have an interesting range of applicability.

The main accomplishment here is the derivation of a simple, but useful, model for two-dimensional, wave-bottom interaction. This model is analysed in various qualitative and quantitative aspects, and predictions stemming from the model are set against observations. The outcome of the comparisons justifies a somewhat sanguine appraisal of the prospects for such models, in spite of the very considerable restriction their use places on the wave and sediment regimes.

The rest of the paper is divided into four Sections. Section 1 is devoted to the derivation of a comparatively simple model that allows for time variations of both free surfaces. The equilibrium configurations of this system are studied in Section 2. A numerical scheme for the integration of the time-dependent equations is presented in Section 3 and used to show that solutions generally evolve into equilibrium formations. The forementioned comparisons between theory and observation are also made in Section 3. Some general commentary and suggestions for further development are given in the concluding Section.

1. The Mathematical Model

When attempting to model wave-bottom interaction it is very helpful to keep observational findings in mind. Especially useful for our purposes is a series of experiments performed in a rectangular channel with a paddle-type wavemaker mounted at one end and an energy absorber at the other. The bottom was laid with sand in various initial configurations before the channel was filled with water. The paddle was then driven at constant frequency and amplitude for many hours, and both the waveform and bedform were monitored over time. A detailed description of these tests is given by Boczar-Karakiewicz, Paplinska and Winiecki (1981), so we content ourselves with a summary of the salient points. The experimental set-up used by Boczar-Karakiewicz et al. (1981), along with a typical equilibrim bed configuration, is pictured in Figure 1.

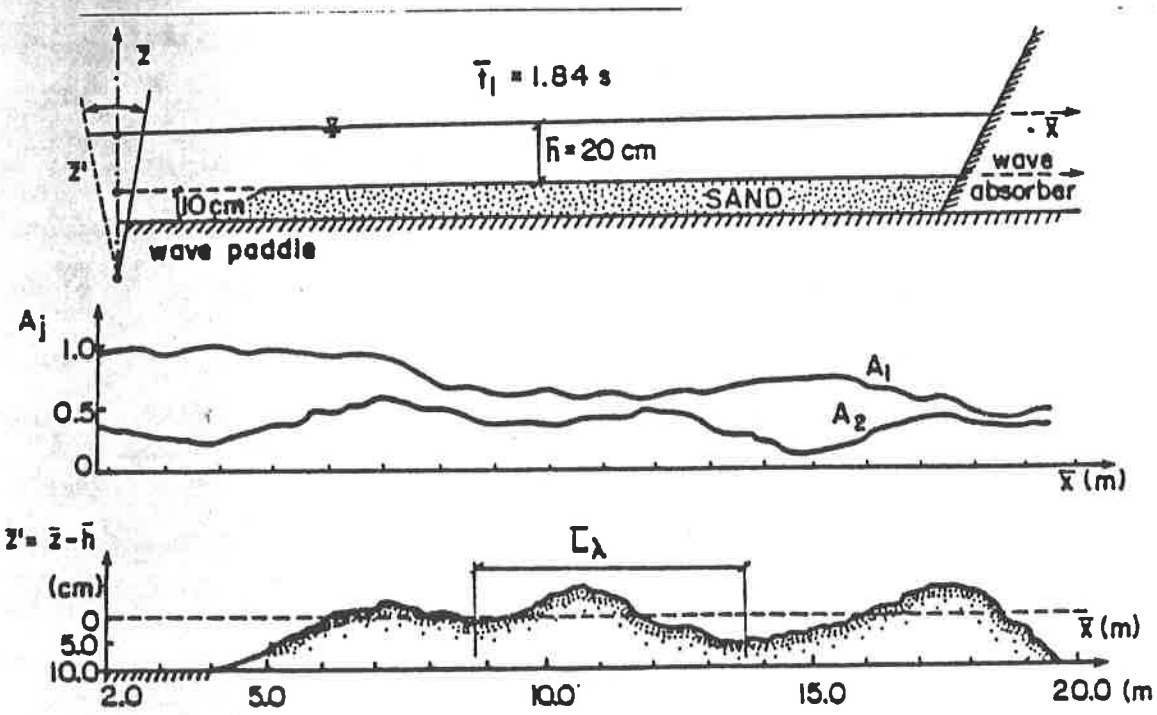

Figure 1. Typical equilibrium bottom profiles in a wave tank experiment:
a) initial bed configuration at T = 0,
b) equilibrium profile at T = 80217 t_1; the A_j are the normalized harmonic amplitudes of the wavefield, j = 1,2, and t_1 is the wave period (after Boczar-Karakiewicz et al., 1981).

The principal point one observes is that in the laboratory scales appertaining to these tests (the flume was 0.5 meters wide, 21 meters long, the water depth was typically 0.3 meters at the wavemaker end, and the wavemaker period was usually about 1.8 seconds) the wave deforms in seconds, whereas the bed experiences significant alteration only over periods of hours. This is not surprising, but it does provide a firm basis for selecting two time scales for the description of the system, one for the evolution of individual waves, and another for the development of the bed. Because of the wide disparity between these two time scales, the bed appears fixed from the viewpoint of an individual wave. In consequence, the modelling may be approached in two stages. In Section 1.1 the wave field is modelled for time intervals that are short enough for the bottom topography to be considered fixed. In Section 1.2 a longer time variable is introduced and used to describe the waves' cumulative effect on the bottom.

1.1 Description of the Wave Field

In the first stage of the modelling, we seek a simple, but sensibly accurate description of a two-dimensional wavetrain as it propagates over a temporally fixed, but spatially variable depth. For the nonce, the spatial region R of interest is, therefore, considered fixed.

We begin by defining the spatial coordinates as follows. Let $\overline{z}$ denote the vertical coordinate, $\overline{x}$ the horizontal coordinate, and let the undisturbed free surface of the liquid be located at $\{(\overline{x},\overline{z}): \overline{z} = 0\}$. Here and in what follows, variables adorned with an overbar are dimensional and unscaled. The surface bounding the liquid from below is taken to be $\{(\overline{x},\overline{z}): = \overline{z} = -\overline{h}(\overline{x})\}$ (see Figure 2). Suppose also that the spatial region R of interest lies in the range where $0 < \overline{x} < \overline{M}$. The point $\overline{x} = 0$ will be identified with the physical point at which the incoming, deep-water wavetrain first comes into the purview of the model. The point $\overline{x} = \overline{M}$ is, in applications, thought of as the point closest to the shoreline where the model is to be applied. It must be emphasized that no attempt is made here to account for the zone very near the water line of a beach. Rather, the present development assumes the waves to be more or less completely dissipated

in the very nearshore region. This point will be amplified later.

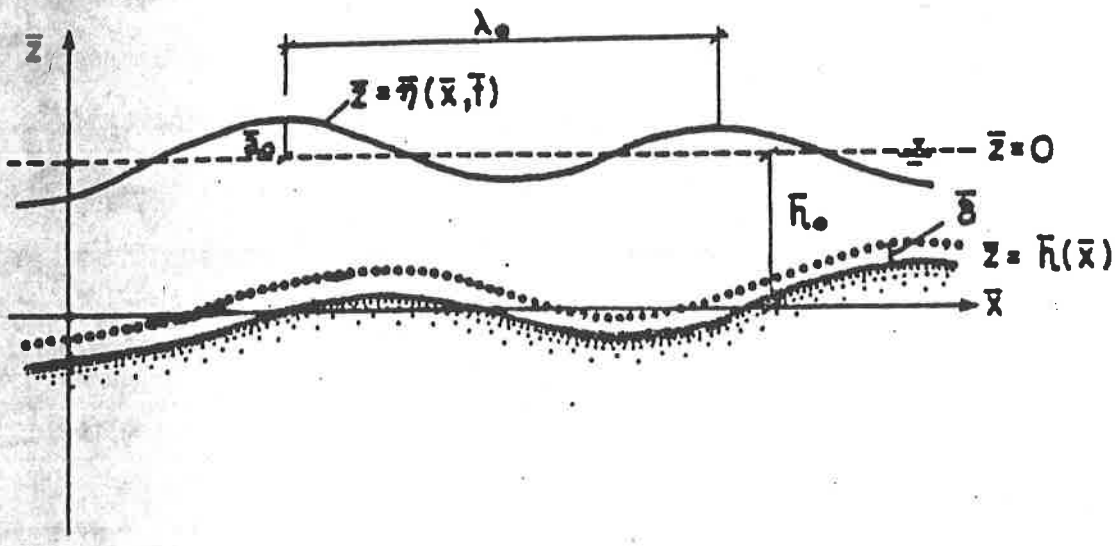

Figure 2. Definition sketch for the two dimensional model: here $\bar{a}_0$ is a typical wave amplitude, λ_0 a typical wave length, $\bar{h}_0$ a typical water depth, $\bar{\delta}$ is the thickness of the boundary layer containing suspended sand, $\bar{z} = -\bar{h}(\bar{x})$ the variable bottom, and $\bar{z} = 0$ denotes the rest position of the free surface of the fluid.

An issue that immediately presents itself is wave breaking. Even on a gently shelving beach, it is not uncommon for incoming progressive waves to break and reform several times. The quantitative description of this process is beyond our present capabilities. However, the experimental data suggests that breaking is not a central ingredient for the sort of bottom structure whose genesis is considered here. For one thing, while the fluid under breakers tends to be more sediment-laden, the general character of the bed deformation there does not appear different than in non-breaking zones (cf. Boczar-Karakiewicz et al. 1981). The sand movement seems to be closely related to the local harmonic content of the flow, especially the first two harmonics. (This is not unexpected since the higher harmonics are not in general energetic enough to move particles on the bottom unless the water is quite shallow; see Section 1.2 below). The evolution of the harmonic content of the wave as it progresses, particularly as regards the fluid motion near the bed, does not appear to be greatly affected by breaking (see

Figure 3). This may be because, if the area very near shore is excepted, breaking only affects the flow catastrophically near the surface; at depth the flow may be quite smooth (cf. Thornton and Schaeffer, 1978). Finally, it has been observed that breaking is not required in the formation of stable structures in a sandy bottom (cf. Benjamin, Boczar-Karakiewicz and Pritchard, to appear).

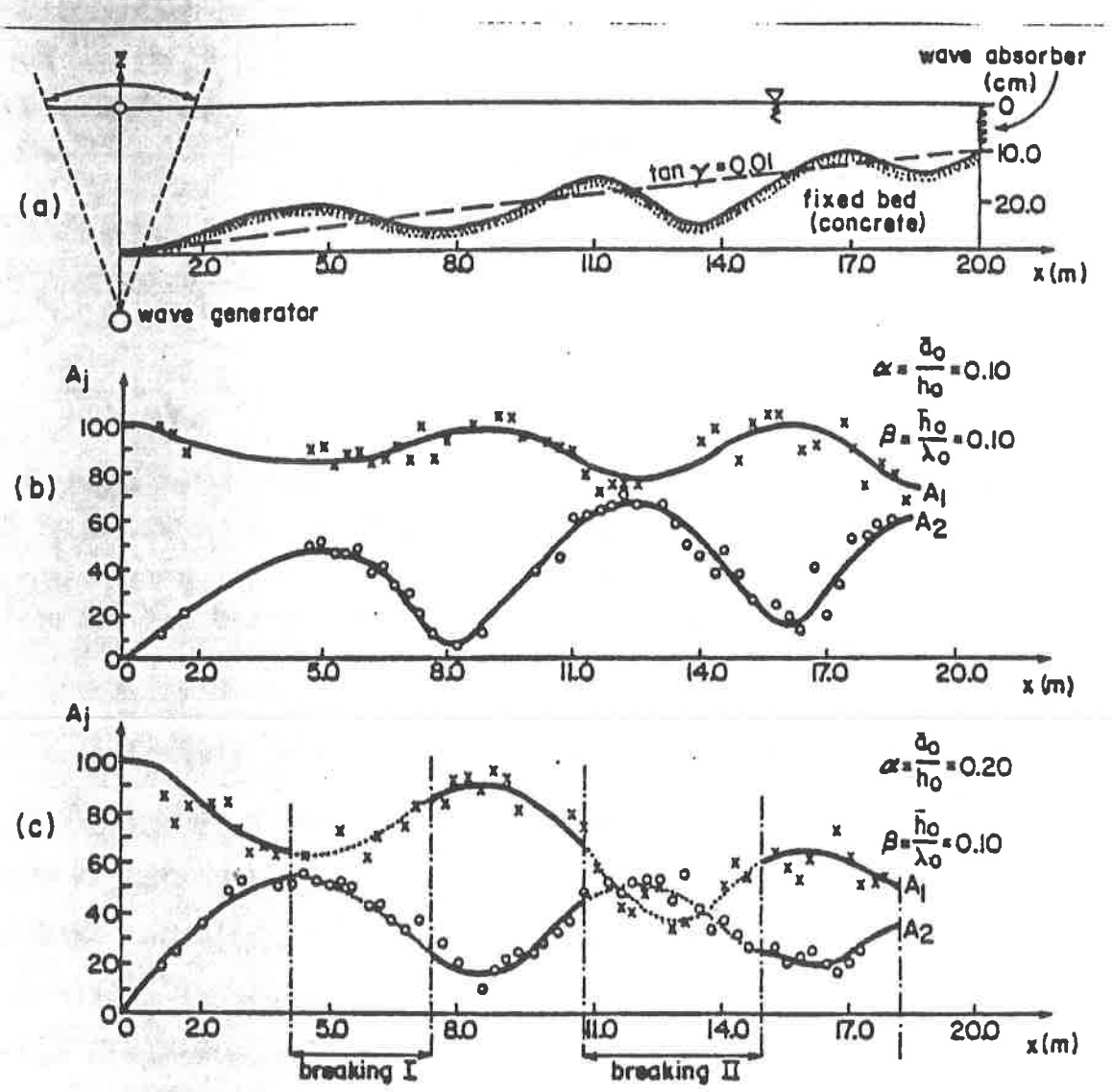

Figure 3. Wave-profile transformation over a fixed bed in a wavetank experiment: (a) experimental configuration, (b) spatial evolution of the two first harmonic amplitudes A_j (j=1,2) of a non-breaking wave, (c) spatial evolution of A_j for a breaking and reforming wave; the harmonic amplitudes A_j are normalized by $A_L^0 = A_j(0)$.

Analysis of the typical scales that obtain on a gradually-sloping beach indicates the shallow-water approximation to the Euler equations as a possible descriptive mode for the wave field (cf. Peregrine 1972, or Whitham 1974). Such a

model is inexpedient because its solutions develop singularities near the shore where the actual wave breaks. Because of this feature, and because of the view enunciated above that breaking is incidental to the process that it is our ultimate interest to describe, we have elected to retain dispersion in the description of the wave motion. The resulting theory is due originally to Boussinesq (1871). It forms a basis for the accounting of the wave field that avoids the singularities inherent in the shallow-water equations. In following this line we are in good company (see e.g. Mei and Méhauté 1966, Madsen and Mei 1969, Lau and Barcilon 1972, Lau and Travis 1973, and Svendsen and Buhr-Hansen 1978).

The Boussinesq approximation to the Euler equations,

$$\bar{u}_{\bar{t}} + g\bar{\eta}_{\bar{x}} + \bar{u}\bar{u}_{\bar{x}} - \frac{1}{3}\bar{h}^2\bar{u}_{\bar{x}\bar{x}\bar{t}} = 0 \,, \qquad (1.1)$$

$$\bar{\eta}_{\bar{t}} + [\bar{u}(\bar{h} + \bar{\eta})]_{\bar{x}} = 0,$$

is derived under the assumptions that nonlinear and dispersive effects are of the same, small order of magnitude and that the bottom varies gradually. Here g is the magnitude of the acceleration due to gravity, $\bar{t}$ is elapsed time, $\bar{\eta}(\bar{x},\bar{t})$ is the vertical deviation of the fluid surface from its undisturbed position at the point $\bar{x}$ at the time $\bar{t}$, and $\bar{u}(\bar{x},\bar{t})$ represents the depth-averaged horizontal velocity of the fluid above the point $\bar{x}$ at the time $\bar{t}$. This system of equations can be put into a variety of other forms by taking different dependent variables and by using the zeroth-order approximation to alter the first-order nonlinear or dispersive corrections; see Bona and Smith (1976), and the references contained therein. Here, it is convenient to work with the following non-dimensional variables;

$$x = \bar{x}/\lambda_0 \,, \quad t = \bar{t}\sqrt{gh_0}/\lambda_0, \quad u = \bar{u}\sqrt{h_0}/a_0\sqrt{g} \qquad (1.2)$$

$$\zeta = \bar{\eta}/a_0, \qquad h = \bar{h}/h_0,$$

where a_0 and λ_0 denote a typical amplitude and wavelength, respectively, in the wavetrain, and h_0 is a representative depth in the region R of interest. In these variables the Boussinesq equations become

$$u_t + \zeta_x + \alpha u u_x - \frac{1}{3} h^2 \beta^2 u_{xxt} = 0,$$

$$\zeta_t + [u(a\zeta + h)]_x = 0, \tag{1.3}$$

where

$$\alpha = \frac{a_0}{h_0}, \qquad \text{and} \qquad \beta = \frac{h_0}{\lambda_0}. \tag{1.4}$$

Define also the parameters

$$\varepsilon = \frac{1}{\alpha} \max_{0 \le x \le \bar{M}} [|h'(x)|, |h''(x)|], \quad \text{and} \quad S_0 = \frac{\alpha}{\beta^2}, \tag{1.5}$$

where $\bar{M} = M/\lambda_0$. In the variables displayed in (1.2), u, ζ, and their partial derivatives with respect to x and t are assumed to be of order one. The formal validity of (1.3) as an approximation to the Euler equations subsists on the assumptions that the fluid is inviscid, irrotational, and incompressible, and the motion is planar, that α, β, and ε are small compared to 1, and that h and S_0 are order one. The Stokes number S_0 (Stokes 1847, Korteweg and de Vries 1895) is a measure of the relative importance of nonlinear and dispersive effects experienced by the wave train. Nonlinear and dispersive effects will contribute to order-one changes in the wave profile on temporal or spatial scales of order α^{-1} and β^{-2}, respectively. If the bulk of the wave motion is only in one direction, say in the direction of increasing x, then a simpler description is available, namely a variable-coefficient, Korteweg-de Vries-type equation (Johnson 1973, Svendsen and Buhr-Hansen 1978),

$$\zeta_t + c\zeta_x + \frac{3}{2}\frac{\alpha}{c}\zeta\zeta_x - \frac{1}{6}\beta^2 h^2 \zeta_{xxt} + \frac{1}{2} c_x \zeta = 0, \tag{1.6}$$

where $c(x) = [h(x)]^{1/2}$. Here, advantage has been taken of the leading-order relation $a_t = -c a_x$ to rewrite the dispersive term $\frac{1}{6}\beta^2 h^2 c \zeta_{xxx}$ appearing in the last-quoted references. As explained by Benjamin et al. (1972), this results in capturing more accurately the full, linearized dispersion relation for surface water waves. In the present study attention will be given exclusively to

progressive waves, and so the just-mentioned simplification would be available. However, at a later stage we expect to allow for small reflection effects and so the level of generality inherent in the Boussinesq equations, the possibility for waves to propagate in two directions, has been retained.

The hypothesis that S_0 is of order one is troublesome. Even on moderately sloping beaches, say a mean slope of 0.5°, the local value of the Stokes number reaches 20 to 30 in regions of interest. As it happens, the Boussinesq-type approximation performs quite accurately in just this sort of regime. As a case in point, reproduced in Figure 4 there is a comparison made by Bona, Pritchard and Scott (1981) of a laboratory observation and an associated numerical solution of essentially equation (1.6) in a regime corresponding to the above-mentioned Stokes number. It should also be noted that this type of approximation is substantially correct even for considerably larger values of S_0 (cf. Zabusky and Galvin 1971, Hammack 1973, Hammack and Segur 1974, Svendsen and Buhr-Hansen 1978).

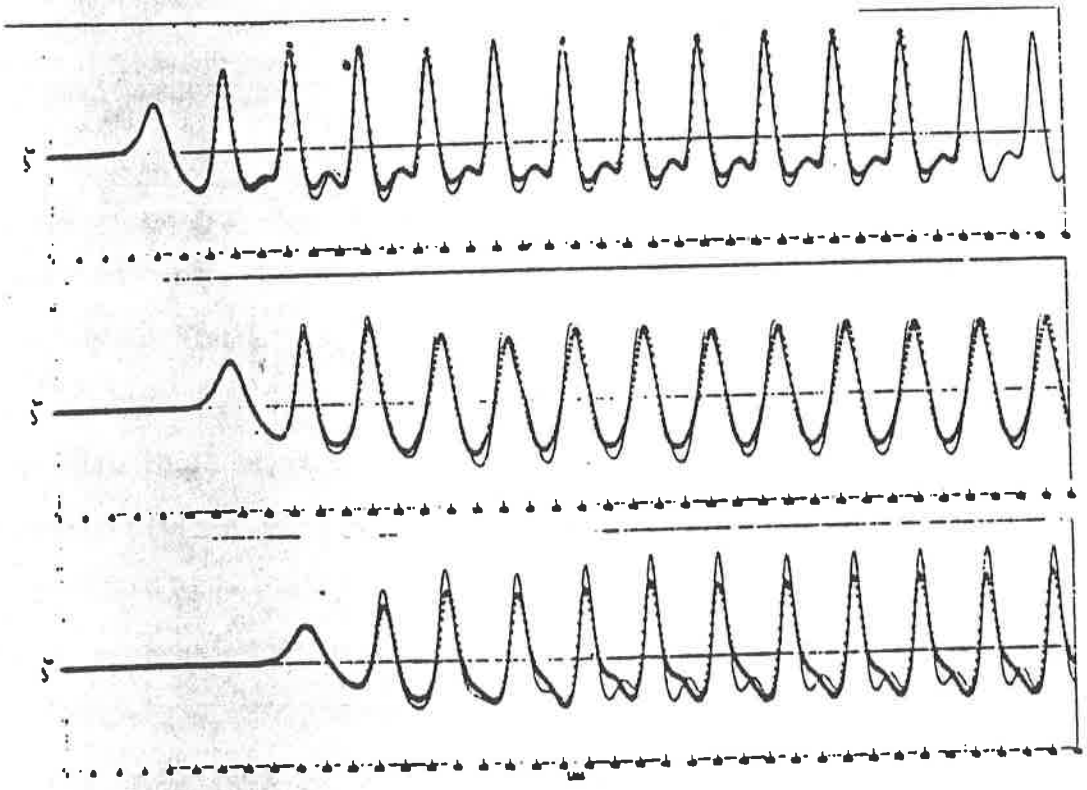

Figure 4. Wave measurements (the diamonds) of waves at Stokes number $S_0 = 26.3$ compared with computed values (the solid lines) of the free surface elevation using a KdV-type model, as a function of time at three different positions in the wavetank (after Bona et al.).

With approximate initial and boundary conditions, the system (1.3) constitutes a well-posed problem. A set of auxilliary specifications that suits the region R is the following:

$$\begin{aligned} &\zeta(x,0) = g_1(x)\ ,\ u(x,0) = g_2(x), \quad \text{for} \quad 0 < x < M, \\ &\zeta(0,t) = \zeta_0(t) \quad \zeta(M,t) = \zeta_1(t), \quad \text{for} \quad t > 0, \\ &u(0,t) = u_0(t) \quad u(M,t) = u_1(t), \end{aligned} \tag{1.7}$$

where g_1, g_2, ζ_0, u_0 and u_1 are given functions. This corresponds to prescribing the surface displacement ζ and velocity distribution u at an initial instant of time, $t = 0$, and at the endpoints of the underlying horizontal domain $\{x: 0 < x < M\}$. For treatments of the well-posedness of (1.3) the reader may consult Schonbek (1978) and Amick (1984). For numerical schemes see Peregrine (1967), Madsen and Mei (1969) and Winther (1979). As regards similar issues for (1.6) wherein only ζ need be specified as in (1.7), see Svendsen and Burh-Hansen (1978), Bona and Dougalis (1980) and Bona, Pritchard and Scott (1981). For neither model is the theory in a completely satisfactory state. Even if g_1 and g_2 are set to zero, on the supposition that the initial wave configuration will have no sensible effect on the long-term status of the system, it is difficult to measure accurately the data exhibited in (1.7). In the field one certainly cannot expect this much information. A more likely provision would be an incoming wave spectrum at a point corresponding to $x = 0$.

For several reasons a further simplification of (1.3) or (1.6) will be carried out. The coarse-grained data that one can expect in a field situation means that the accuracy attained using (1.3) or (1.6) is somewhat illusory. Moreover, it must be remembered that the present model will be coupled to a model for the deformation of the bed in Section 1.2. In numerically approximating the equations for the liquid and sediment surfaces it will be required to predict the waveform many times during the slow evolution of the bedform. Consequently, while it is true that (1.3) can be efficiently integrated numerically, the computation becomes extensive when the erosion of the bed is considered. Finally, the forthcoming simplification has the salutory effect of allowing the use of analytic techniques to answer certain questions.

In the reduction to be effected now we explicitly follow the lead of Lau and Barcilon (1972) (see also Armstrong et al. 1962, and Mei and Ünlüata, (1972). The clue to this step is already evident in Figure 3, which emphasizes the relationship between the waves and their first few harmonic components. Assume now that the wave incident at the 'deep-water' end, x = 0, is a single-frequency, planar, steadily-propagating linear wavetrain. This presumption corresponds closely to the experimental conditions maintained by Boczar-Karakiewicz et al. (1981) cited earlier. It is also reasonably veritable on some real beaches. As an example there is shown in Figure 5 a representative energy density distribution measured off a Baltic Sea coast by Druet, Massel and Zeidler (1972). (Similar observations are reported by Guza and Thornton, 1980 and Elgar and Guza, 1984), using measurements obtained on a California beach.) Note especially the deep-water spectrum (solid line) that is sharply peaked about a single frequency ω_1 corresponding to a period of about 7 seconds. In this particular instance the

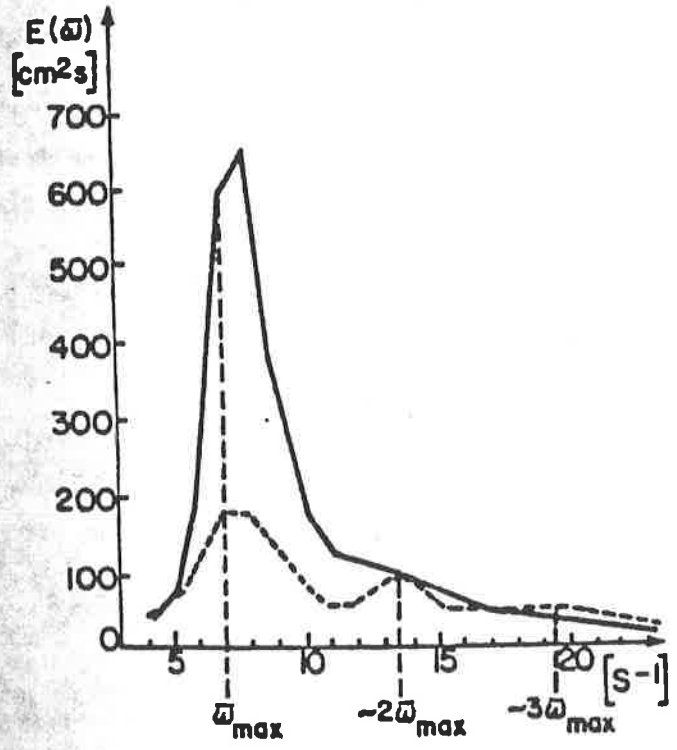

Figure 5. Energy density distribution off the coast of the Southern Baltic Sea: - offshore measurements ($\overline{h}_0$ = 6.00 m), --- nearshore measurements ($\overline{h}_0$ = 2.00 m).

waves were propagating normal to the beach and bathymetry showed that the assumption of the waves two-dimensionality was valid. As the waves propagated shoreward,

there transpired a pronounced shift of energy to the second harmonic frequency, $\omega_2 = 2\omega_1$, (dashed line in Figure 5). This accords nicely with predictions we shall make later.

In agreement with the assumptions leading to (1.3), the bottom configuration h is taken to have the slowly-varying form

$$h(x) = 1 + \varepsilon f(x), \tag{1.8}$$

for $0 < x < M$, where ε is the small parameter defined in (1.5). Since h has order one, we may take it that f has order one. However, (1.5) implies that $f'(x)$ has order α. Because of this, it is indicated to introduce a new horizontal variable X defined by

$$X = \alpha x.$$

Let $F(X) = f(X/\alpha)$. Then the foregoing assumptions concerning f and ε imply that h has the form

$$h(X) = 1 + \varepsilon F(X), \tag{1.9}$$

where F and F' are both of order one, and ε is small compared to unity.

Following Lau and Barcilon (1972) a two-scale expansion will be introduced, treating x and X as independent variables. For this to be effective a decision regarding the relative sizes of the three small parameters α, β, and ε must be rendered. It will be presumed they all three have the same small size since this is in fact the case in many near-coastal areas.

This latter assumption has associated theoretical difficulties which are now explained. The supposition that ε/α is of order one presents no problem. But if α/β has order one, then the Stokes number $S_0 = \alpha/\beta^2$ has order $1/\beta$, and so is representative of a regime in which nonlinear effects predominate. Thus the specified scalings appear contradictory, and indeed a proper limiting procedure appropriate for (1.3) in which, say,

$$\varepsilon, \alpha, \beta \to 0, \quad \text{with} \quad S_0 \quad \text{and} \quad \frac{\varepsilon}{\alpha} \text{ fixed},$$

would lead to a singularity in the forthcoming model. (This point is not empha-

sized in the earlier work of Lau and Barcilon 1972). The model will not be applied in such a limiting case, however, but rather to situations involving finite values of the parameters α, β, and ϵ. For the usual sort of values of β the difference between the variable X and the variable $Y = \beta^2 X$ more naturally associated with (1.3) is the moderate-sized multiplicative constant S_0. Looking ahead to the way in which X enters in the model, it becomes apparent that the choice in (1.8) is not crucial so long as fixed finite values of the parameters are in question. In fact, this choice of scales corresponds to assumptions, intermediate between those leading to the Boussinesq equations and those leading to nonlinear shallow-water theory, that emphasize nonlinearity, but do not ignore dispersion entirely. Presumably what is important is how accurately the overlying equation (1.3) or (1.6) predict wave phenomena in the regime that corresponds to a particular set of parameter values. The previously-quoted work of Svendsen and Buhr-Hansen (1978) and Bona, Pritchard, and Scott (1981) seems to assure that for the range of parameter values of utmost interest for the present study (α, β, ϵ about 0.10, S_0 in the range 10 to 30) the models predict rather well. (It should be acknowledged that the good agreement between numerical predictions and the outcome of laboratory measurements obtained in the just-referenced papers subsisted in part on appending to the model a dissipative mechanism. For laboratory-scale experiments there is little doubt that dissipation from the boundary layers and other sources is quite important. On field scales these effects are much less important, and so are ignored here. They will be incorporated in subsequent, more refined studies.)

Proceeding with the two-scale expansion, if r is a function of x and X, then by the chain rule,

$$\frac{d}{dx} r(x,X) = \frac{\partial r}{\partial x} + \alpha \frac{\partial r}{\partial X} . \qquad (1.10)$$

The relationship embodied in (1.10) is maintained even when x and X are treated as independent variables. Suppose the incoming wave-train is periodic with a frequency ω_1. The normal modes associated to the linearized Boussinesq equations ((1.3) with $\alpha = 0$) which propagate in the direction of increasing x are

$$e^{i(k_j x - \omega_j t)},$$

where $\omega_j = j\omega_1$ and $k_j > 0$ is determined by the linearized dispersion relation

$$\omega_j^2 = \frac{k_j^2}{1 + \frac{\beta^2}{3} k_j^2}. \tag{1.11}$$

In the absence of nonlinearity the general periodic solution of (1.3) propagating in the $+x$ direction would be represented as a linear combination of the normal modes. To take account of nonlinearity, the coefficients in the normal-mode decomposition are allowed to vary. Keeping in mind that nonlinear effects acumulate over time scales of order α^{-1}, it is natural to assume that the coefficients vary on the spatial scale embodied in the variable X. Hence, we write

$$\zeta(x,X,t) = \sum_j \zeta_j(X) e^{i(k_j x - \omega_j t)} + \text{c.c.},$$

and

$$u(x,X,t) = \sum_j u_j(X) e^{i(k_j x - \omega_j t)} + \text{c.c.}, \tag{1.12}$$

where we are following the usual method of representing a real function in terms of complex exponentials by letting c.c. stand for the complex conjugate of the sum it follows. As ζ and u are of order one, so are the coefficients ζ_j and u_j. On the basis of both field and laboratory measurements, attention is restricted to the first two harmonics, $j = 1,2$ (see again Figures 1,3 and 5). The resulting finite expansions are substituted into (1.3) and only terms containing modes of the frequency ω_1 or ω_2 are retained, the others being assumed negligible. Keeping in mind the relation (1.10), and writing

$$h(X) = 1 + \alpha G(X), \tag{1.13}$$

where $G(X) = \frac{\varepsilon}{\alpha} F(X)$, we obtain

$$u_t + \zeta_x - \frac{\beta^2}{3} u_{xxt} = -\alpha\zeta_X - \alpha u u_x + \frac{2\zeta\beta^2}{3} G u_{xxt}$$

$$+ \frac{2\beta^2\alpha}{3} u_{xXt} + \text{order } (\alpha^2), \tag{1.14}$$

$$\zeta_t + u_x = - \alpha u_X - \alpha(u\zeta)_x - \alpha G u_x + \text{order } (\alpha^2) .$$

From the second equation in (1.14) and assumptions (1.12) it is deduced that

$$u_j(X) = \frac{\omega_j}{k_j} \zeta_j(X) + \text{order } (\alpha), \tag{1.15}$$

for $j = 1,2$. The variable ζ may be eliminated from the left-hand side of these equations, so coming to the single relation

$$u_{tt} - u_{xx} - \frac{\beta^2}{3} u_{xxtt} = \alpha\{- \zeta_{Xt} + u_{Xx} + G u_{xx} +$$

$$\frac{2\beta^2}{3} [G u_{xxtt} - u_{xXtt}] - \frac{1}{2} (u^2)_{xt} + (\zeta u)_{xx}\} + \text{order } (\alpha^2) . \tag{1.16}$$

Note that whilst β is viewed as fixed and non-negligible relative to one, so dispersive effects enter, it is nevertheless small. Hence the dispersion relation (1.11) implies that $\omega_j \cong k_j$, $j = 1,2$, which in turn suggests that $k_2 - 2k_1 = \omega_2 - 2\omega_1 + \Delta k = \Delta k$ is small (it is of order β^2). Thus the variable $x\Delta k = (\Delta k/\alpha)X$ may be taken as comparable with X, and so independent of x. In equation (1.16) the terms of order α^2 are ignored, as are all temporal harmonics except ω_1 and ω_2. With these provisos, and because the first two harmonics are linearly independent, equation (1.16) means that the coefficients of the first two harmonics must each vanish. The result of this requirement is the Lau-Barcilon equations,

$$\zeta_1'(X) + iF_1\zeta_1(X) + iQ_1 e^{i\tilde{\Delta}kX} \zeta_1^*(X)\zeta_2(X) = 0,$$

$$\zeta_2'(X) + iF_2\zeta_2(X) + iQ_2 e^{-\tilde{\Delta}kX} \zeta_1^{\,2}(X) = 0, \tag{1.17}$$

where $*$ denotes complex conjugation,

$$F_j = \frac{k_j^{\,3}}{2\omega_j^{\,2}} (1 - \frac{2\beta^2}{3} \omega_j^{\,2})G(X), \quad j = 1,2,$$

$$Q_1 = (k_2 - k_1)(\frac{k_1}{k_2\omega_1})[\omega_1 + (k_2 - k_1)(\frac{k_2}{\omega_2} + \frac{k_1}{\omega_1})],$$

$$Q_2 = \frac{k_2^{\,2}}{8k_1} (1 - \frac{2k_1^{\,2}}{\omega_1^2}), \tag{1.18}$$

and $\tilde{\Delta k} = \frac{\Delta k}{\alpha}$.

In deriving (1.17), repeated use of (1.15) has been made. Since (1.15) is applied to terms that are of order α, the error implicit in its use is of order α^2, and so is neglected in the approximation considered here. Note that discarding terms of order α^2 is consistent with the use of (1.3). Notice also that $\tilde{\Delta k}$ is of order $1/S_0$.

The representation (1.12) coupled with the Lau-Barcilon equations (1.17) and the relation (1.15) comprise our description of the wave field over a fixed, gradually-varying bottom. It is formally valid for times that are short compared to those over which the bed topography deforms.

The Lau-Barcilon equations must be supplemented with the appropriate analog of the auxilliary data (1.7). Because reflection has been ignored the boundary condition at $x = M$ is dispensible. The initial data has implicitly been set to zero and it is only necessary to account for the conditions at $x = 0$. Because of (1.15) it suffices to specify $\zeta(0,t)$, since $u(0,t)$ is then inferred. The assumed form (1.12) entails only the first two harmonics and consequently we need only specify the projection of $\zeta(0,t)$ onto these harmonics. That is, if

$$\zeta(0,t) = \sum_{j=1}^{\infty} a_j^0 e^{i\omega_j t} + \text{c.c.},$$

then our presumption is that a_j is negligible for $j > 3$. Hence it is taken that

$$\zeta(0,t) = a_1^0 e^{i\omega_1 t} + a_2^0 e^{i\omega_2 t} + \text{c.c.},$$

whereupon the equations in (1.17) are to be solved subject to

$$\zeta_1(0) = a_1^0 , \quad \zeta_2(0) = a_2^0. \tag{1.19}$$

A special case that corresponds to the experimental and field data described earlier obtains when $a^0 = 1/2$ and $a^0 = 0$, so that $\zeta(0,t) = \cos(\omega_1 t)$.

In using the model for the wave field described above, it is often convenient

to return to the variable x throughout, the 'long' variable X having served its purpose. To this end define

$$a_j(x) = \zeta_j(X), \quad \text{for } j = 1,2. \tag{1.20}$$

Then formulae (1.17 - (1.18) may be written in the useful form,

$$\begin{aligned} a_1'(x) + i\varepsilon f_1 f(x) a_1(x) + i\alpha Q_2 e^{i\Delta k x} a_1^*(x) a_2(x) &= 0, \\ a_2'(x) + i\varepsilon f_2 f(x) a_2(x) + i\alpha Q_2 e^{-i\Delta k x} a^2(x) &= 0, \end{aligned} \tag{1.21}$$

where, for $j = 1,2$,

$$f_j = \frac{k_j^3}{2\omega_j^2}\left(1 - \frac{2\beta^2}{3}\omega_j^2\right), \tag{1.22}$$

Q_1 and Q_2 are defined in (1.18), f is defined in terms of h in (1.8), and $\Delta k = k_2 - 2k_1$ as before. The boundary conditions (1.19) apply without change to the system (1.21).

1.2 Description of the Bottom Deformation

Still considering the bottom configuration as fixed and known, and assuming a_1 and a_2, and thereby ζ and u, to be determined, it is possible to infer the fluid velocity near the bed from inviscid theory. The horizontal velocity U at a depth z below the undisturbed free surface is, to the accuracy afforded by the approximations made in deriving the Boussinesq equations, given by the formula

$$U(x,t;z) = u(x,t) - \beta^2\left[\frac{1}{3}h^2(x) - zh(x) - \frac{1}{2}z^2\right]u_{xx}(x,t),$$

(cf. Peregrine, 1972). Define u_b to be the horizontal component of the fluid velocity at $z = -h(x)$. Then it follows that

$$u_b(x,t) = u(x,t) - \frac{\beta^2}{6}h^2(x)u_{xx}(x,t). \tag{1.23}$$

Using (1.12) and (1.15), u_b may be expressed in terms of a_1 and a_2 as

$$u_b(x,t) = \sum_{j=1}^{2} \frac{\omega_j}{k_j} \left(1 - \frac{\beta^2}{6} h^2(x) k_j^2\right) a_j(x) e^{i(k_j x - \omega_j t)} + \text{c.c.} \qquad (1.24)$$

The view is taken that the layer of fluid near the bottom is viscous and sediment-laden. Let $\bar{\delta}$ denote the thickness of this layer, and assume that $\bar{\delta} < h_0$. It is our purpose now to analyse the sediment movement in this boundary layer. The overall instantaneous deformation of the bed will then be identified with the differential movement of the sediment within the bottom layer of fluid. (This very simple model is ideal to illustrate principles. More realistic models for the sediment transport will be reported in subsequent studies of this general model).

To provide a basis for our discussion, it is worth reporting some detail of the laboratory observations of Boczar-Karakiewicz et al. (1981) in regard to the sediment movement. Very soon after subjecting an initially flat bed of sand to periodic wave motion, small scale ripples appear in the bed. The oscillatory motion of the fluid over such ripples generates small patches of vorticity that are very effective at lifting the sand from the bed (Sleath, 1978). These small-scale ripples persist, and from their inception onward there is a plentiful supply of sand in the lower reaches of the fluid. (An idealized analysis of an oscillating flow over a ripply bed has been given recently by Longuet-Higgens, 1981).

In the analysis to follow, no attempt will be made to describe the process whereby the sediment is suspended in the fluid. Rather, a distribution of sediment in the boundary layer will simply be postulated. It transpires that the resulting model is not highly sensitive to the assumed sediment distribution, and the boundary layer depth can be scaled out of the model equations.

As a first approximation the suspended particles are presumed to be transported with a velocity proportional to that of the ambient fluid, and their influence on the flow is neglected. Hence interest naturally turns to the mass-transport velocity of the fluid near the bed. The approach taken to the mass-transport velocity is based on the seminal work of Longuet-Higgens (1953). The general idea, recognized already by Stokes (1847), is that fluid-particle orbits

generated by the propagation of finite-amplitude waves are not closed. Repeated passage of progressive waves therefore engenders a small drift velocity, called the mass-transport velocity.

As the suspended sediment is concentrated near the bed, and since under our assumptions a purely oscillatory motion would produce no mean movement of the sediment, it is the mass-transport velocity in the lower reaches of the fluid that is central. This is exactly what was studied by Longuet-Higgens in the setting of Stokes' waves over a laminar, viscous boundary layer. His methods carry over intact for the shallow-water waves of interest here. Of course, the motion near the bed is really turbulent, as the description of the experimental observations suggests. In such a situation the mean aspects of the motion could be described by way of a coefficient of eddy viscosity whose value varies with distance from the boundary. Using this sort of idea in the context of Stokes' waves, Johns (1970), showed that for both standing and progressive waves the predictions of the model only differed by a multiplicative factor from the description obtained via laminar boundary-layer theory. Such differences may be taken into account by applying the laminar theory with an eddy viscosity that is 10 to 100 times the ordinary kinematic viscosity.

We begin the analysis by concentrating attention around a particular point x on the horizontal scale. Longuet-Higgins' development simplifies considerably, because near x the bed may be treated as horizontal and without curvature on account of the assumption that the parameter ε defined in (1.5) is of order α. In addition to the horizontal coordinate x, the stretched variable

$$n = \frac{z + h(x)}{\delta} , \tag{1.25}$$

where

$$\delta = \left[\frac{\bar{\nu}}{h_0 (g h_0)^{1/2}} \right]^{1/2} \frac{\bar{\delta}}{h_0} , \tag{1.25}$$

is used to describe the boundary layer. Here δ is a dimensionless boundary-layer thickness and ν refers to an appropriate, dimensional eddy viscosity. Observations in the laboratory indicate that typical values of δ are about 0.05.

Consideration is given to the mean horizontal velocity $U(x,n,t)$ in the boundary layer n units above the bed at x at time t. In the approximation afforded by the use of an eddy viscosity it is found (see Longuet-Higgins, 1953, formula (155)) that

$$[\beta \frac{\partial}{\partial t} - \frac{\partial^2}{\partial n^2}]u = \beta \frac{\partial u_b}{\partial t}, \tag{1.26}$$

where, as in (1.24), u_b is the horizontal velocity at the bottom of the inviscid layer. Naturally, U satisfies the no-slip condition at $n = 0$, and must essentially agree with u_b for large values of n which correspond to the top of the viscous layer. The form of u_b in (1.24) compels the ansatz that

$$U(x,n,t) = \sum_{j=1}^{2} P_j(x,n)e^{i(k_j x - \omega_j t)} + c.c. \tag{1.27}$$

If the latter relation is substituted into (1.26), there results the equations

$$(- i\omega_j\beta - \frac{\partial^2}{\partial n^2})P_j = - i\beta \frac{\omega_j^2}{k_j} [1 - \frac{\beta^2}{6} h^2(x)k_j^2]a_j(x), \tag{1.28}$$

for $j = 1,2$. The general solution of these ordinary differential equations is

$$P_j(x,n) = S_j(x)e^{\Lambda_j n} + T_j(x)e^{-\Lambda_j n} + \frac{\omega_j}{k_j} [1 - \frac{\beta^2}{6} h^2(x)k_j^2]a_j(x),$$

where

$$\Lambda_j = (1 - i)(\frac{\omega_j \beta}{2})^{1/2},$$

for $j = 1,2$, and the positive square root is meant. Since P_j must tend to the corresponding coefficient of u_b for large n and to 0 as n tends to 0, it is determined that

$$U(x,n,t) = \sum_{j=1}^{2} \frac{\omega_j}{k_j} [1 - \frac{\beta^2}{6} h^2(x)k_j^2]a_j(x)[1 - e^{-n\Lambda_j}]e^{i(k_j x - w_j t)} + c.c. \tag{1.29}$$

With U in hand, the mass-transport velocity in the boundary layer is easily computed. First note that if U is averaged over a fundamental period

$t_1 = 2\pi/\omega_1$, we obtain zero. This is the usual state of affairs for small-amplitude waves, in which there are no first-order currents. For the drift velocity one must look to the next order, as Stokes (1847) already appreciated. At the second order the average over a period t_1 gives the lowest-order approximation of the mass-transport velocity u_m, and is not usually zero. In fact, Longuet-Higgins has determined its value generally, under assumptions weaker than those in force here. In our variables, this has the form

$$u_m(x,n,t) = 4 \int_t^{t+t_1} [\frac{\partial u_b}{\partial x}(x,t) \int_0^\tau U(x,n,s)ds]d\tau$$
$$+ 3\int_0^n \int_t^{t+t_1} \{[\frac{\partial U}{\partial x}(x,n',\tau) - \frac{\partial u_b}{\partial x}(x,t)] \int_0^\tau \frac{\partial U}{\partial n}(x,n',s)ds\}d\tau dn', \tag{1.30}$$

(see Longuet-Higgins, 1953, formula (169)). Using the previously obtained expressions for U and u_b, the mass-transport velocity, u_m, may be evaluated explicitly as

$$u_m(x,n) = \sum_{j=1}^{2} \frac{\omega_j}{k_j} |a_j(x)|^2[1 - \frac{\beta^2}{6} h^2(x)k_j^2]^2 \tilde{D}_j(\delta), \tag{1.31}$$

where

$$\tilde{D}_j(\delta) = 5 - 8e^{-\mu_j}\cos(\mu_j) + 3e^{-2\mu_j},$$

with (1.32)

$$\mu_j = n(\frac{\beta\omega_j}{2})^{1/2} = \frac{1}{\delta} z(\frac{\beta\omega_j}{2\delta})^{1/2}.$$

Note that U_m is independent of the fast time variable t. In obtaining (1.31) we have ignored the small quantities $h'(x)$ and $a_j'(x)$ in favour of the order-one terms retained above (and, as before, the terms multiplied by β^2 arising from dispersion are inconsistently kept). This would be mechanical if we had maintained the distinction between x and the 'slow' spatial variable X introduced in Section 1.1.

The goal in view now is to determine how the depth changes with time. In the present, very simplified model the temporal evolution of the depth will be intima-

tely connected with the mass-transport velocity, u_m. As determined above, u_m depends directly on the vertical coordinate n in the bottom fluid layer, and on the horizontal coordinate x and time through a_1, a_2, and h. Moreover, a_1 and a_2 depend on time only through variation of h over time. Introduce another, temporal variable T which is such that significant changes in the bed profile take place over time scales T of order one. From the observational data we know that the time variable t representative of a wave period is essentially infinitesimal with regard to T. The depth h is now explicitly allowed to depend on time, but only through the very slow variable T, which is viewed as independent of t. Because $h = h(x,T)$, the amplitudes a_1 and a_2 also depend on T, as does the mass-transport velocity u_m. Of course ζ and u have a dependence on T induced by that of a_1, a_2, and h.

Consider a short time interval, say in which t varies by order one, $[T,T+\Delta T]$, and a small spatial interval $[x,x+\Delta x]$. Let $\rho(n)$ denote the assumed form of sediment density in the lower fluid. (For simplicity, ρ is taken to be identically zero outside the lower layer.) A typical distribution, having some theoretical justification (cf. Raudkivi, 1976), is the exponential form, $\rho(n) = \rho_0 e^{-\gamma n}$. A cruder assumption is to simply take the density to be constant in the lower layer, say set at some appropriate average value, $\rho(n) \equiv \bar{\rho}$. In any case, define

$$M(x,T) = \int_0^\infty \rho(n) u_m(x,n,T)\,dn. \tag{1.33}$$

Because of the assumption that the suspended sediment follows the fluid motion, the quantity

$$\int_T^{T+\Delta T} [M(x,\tau) - M(x+\Delta x,\tau)]\,d\tau \tag{1.34}$$

is proportional to the total mass accumulation in the region $I = \{x' : x < x' < x + \Delta x\}$ during the interval $[T,T+\Delta T]$. Since the concentration of suspended sediment is time and space invariant, this mass accumulation must be reflected in the differential amount of sediment on the bed, namely

$$\rho_0 \int_x^{x+\Delta x} [h(x',T+\Delta T) - h(x',T)]\,dx', \tag{1.35}$$

where ρ_0 is the average density of the deposited sediments (the fact that the layer of sediment near the surface of the bed is a saturated porous medium is ignored here). Let K be the constant of proportionality to which allusion was made above (1.34). Then our mass balance has the form

$$K \int_T^{T+\Delta T}[M(x,\tau) - M(x+\Delta x,\tau)]d\tau \tag{1.36}$$

$$= \rho_0 \int_x^{x+\Delta x}[h(x',T+\Delta T) - h(x', T)]dx'.$$

Upon dividing by $\Delta x \Delta T$ and taking the limit formally as Δx and ΔT approach zero, the instantaneous version of the mass balance appears, namely

$$\frac{\partial h}{\partial T} = \frac{K}{\rho_0}\frac{\partial M}{\partial x} = K \int_0^{\infty} \frac{\rho(n)}{\rho_0} \frac{\partial u_m}{\partial x}(x,n,T)dn. \tag{1.37}$$

Again for the sake of simplicity we shall henceforth take $\rho(n) \equiv \bar{\rho}$, though such an assumption is not needed to proceed. Absorbing the dimensionless quantity $\bar{\rho}/\rho_0$ into K, and setting

$$U_m(x,T) = \frac{1}{\delta} \int_0^{\delta} u_m(x,n,T)dn, \tag{1.38}$$

(2.37) becomes

$$\frac{\partial h}{\partial T} = \tilde{K}\frac{\partial U_m}{\partial x} \quad \text{where} \quad \tilde{K} = \delta K. \tag{1.39}$$

The variable U_m is readily evaluated in terms of a_1 and a_2 to be

$$U_m(x,T) = \sum_{j=1}^{2} \frac{\omega_j}{k_j} |a_j(x,T)|^2[1 - \frac{\beta^2}{6} h^2(x,T)k_j^2]^2 D_j, \tag{1.40}$$

where

$$D_j = 5(1 - \frac{1}{2v_j}) - 3\frac{e^{-2v_j}}{2v_j} + 4\frac{e^{-v_j}}{v_j}(\cos v_j - \sin v_j)$$

and

$$v_j = (\frac{\beta\omega_j}{2})^{1/2}, \text{ for } j = 1,2. \tag{1.41}$$

The reader will note that after $\mathcal{K}$ replaces K in (1.39), the boundary layer depth no longer appears explicitly in our formulas. In effect, the timescale T can be rescaled to eliminate δ from the model equations, a potentiality that has been exercised throughout the remainder of this paper.

The simple law (1.39) combined with the Lau-Barcilon equations (1.21) and supplemented by the original bottom configuration,

$$h(x,0) = H(x), \tag{1.42}$$

for $0 < x < M$, serves to determine the bed profile for $T > 0$.

In summary, the model suggested here has the general form

$$\begin{aligned} \frac{\partial a_1}{\partial x} &= A_1(a_1, a_2, h), \\ \frac{\partial a_2}{\partial x} &= A_2(a_1, a_2, h), \\ \frac{\partial h}{\partial T} &= H(a_1, a_2, h), \end{aligned} \tag{1.43}$$

where the functions A_1 and A_2 are defined in formulae (1.18), (1.21), and (1.22), and H is defined in (1.39), (1.40), and (1.41). The system (1.43) is supplemented by the auxilliary conditions

$$\begin{aligned} a_1(0,T) &= a_1^0, \\ a_2(0,T) &= a_2^0, \end{aligned} \tag{1.44}$$

for $T > 0$, as in (1.19), corresponding to a fixed, incoming, deep-water wavetrain, and

$$h(x,0) = H(x), \tag{1.45}$$

as in (1.42), corresponding to a given initial bed profile. Whilst several somewhat drastic simplifications have been made in the construction of this model, we shall see that the model still retains what appears to be certain of the fundamental elements of wave-bottom interaction. Moreover, the model seems to have

predictive power, even in its present, preliminary stage of development.

2. Equilibrium Configurations

Since one of our principle aims is to explain in some measure the formation of stable bed structures in near-shore zones, it is natural to consider what kind of time-invariant solutions are possessed by the model developed in the last Section. Before embarking on a tudy of equilibrium solutions, it is useful to understand certain general aspects of the equations more fully.

As in the derivation, attention is given first to the situation wherein the bed is fixed. In this case we are concerned only with the Lau-Barcilon equations (1.21). As noticed by Armstrong et al. (1962), this system of equations admits a conservation law, namely

$$E = \frac{|a_1(x)|^2}{\alpha Q_1} + \frac{|a_2(x)|^2}{\alpha Q_2} . \tag{2.1}$$

That is, for all $x > 0$, $E(x) = E(0)$, and so E is determined by the initial data (1.19) for the incoming wavefield.

Consider first that the bed is flat and horizontal, so that $h(x) \equiv 1$ and $f(x) \equiv 0$. The system (1.21) simplifies to

$$\begin{aligned} a_1'(x) + i\alpha Q_1 e^{i\Delta k x} a_1^*(x) a_2(x) &= 0, \\ a_2'(x) + i\alpha Q_2 e^{-i\Delta k x} a_1^2(x) &= 0, \end{aligned} \tag{2.2}$$

for $0 \leq x \leq M$, with

$$a_1(0) = a_1^0, \qquad a_2(0) = a_2^0.$$

In this form the equations admit an exact solution, given already by Armstrong et al. (1962, see also Mei and Ünlüata, 1972). The salient results are merely reported here. Temporarily define new variables as follows:

$$E_0 = \frac{|a_1^0|^2}{\alpha Q_1} + \frac{|a_2^0|^2}{\alpha Q_2} , \tag{2.3}$$

$$w(x) = \frac{|a_1(x)|}{(\alpha E_0 Q_1)^{1/2}}, \qquad v(x) = \frac{|a_2(x)|}{(\alpha E_0 Q_2)^{1/2}}, \tag{2.4}$$

and

$$\tilde{x} = \alpha Q_1 (\alpha Q_2 E_0)^{1/2} x. \tag{2.5}$$

View v and w as functions of $\tilde{x}$ rather than x. Then the conservation of energy expressed in (2.1) becomes

$$w^2(x) + v^2(x) = 1. \tag{2.6}$$

The solution of (2.2), expressed in the variables given in (2.3)-(2.5), is

$$v^2(\tilde{x}) = v_a^2 + (v_b^2 - v_a^2)\,sn^2[(v_c^2 - v_a^2)^{1/2}(\tilde{x} - \tilde{x}_a);\ \gamma], \tag{2.7}$$

$$w^2(x) = 1 - v^2(x),$$

where sn denotes the Jacobian elliptic function, $v_a^2 < v_b^2 < v_c^2$ are the three real roots of the cubic equation

$$0 = P(v^2) = (1-v^2)v^2 - [\Gamma + \tfrac{1}{2}\Delta Q(v^2 - v^2(0))],$$

with

$$\Delta Q = \frac{\Delta k}{\alpha Q_1 (\alpha Q_2 E_0)^{1/2}},$$

$$\Gamma = w^2(0)v(0)\cos(\theta(0)),$$

and the modulus γ of sn has the value

$$\gamma = \left(\frac{v_b^2 - v_a^2}{v_c^2 - v_a^2}\right)^{1/2}.$$

The parameters governing this solution, Γ, ΔQ, $v(0)$, $w(0)$, $\theta(0)$, and $\tilde{x}_a$ are inter-related in easily determined ways, so that only three are free, and these comprise a constrained set within themselves. The exact forms of these constraints is not important here, but what is interesting is that the first and second harmonics both vary periodically in space with period

$$\tilde{L}_\lambda = \frac{2K}{(v_c^2 - v_a^2)^{1/2}}$$

in the $\tilde{x}$ variable, where K is the complete elliptic integral

$$K = K(\gamma) = \int_0^{\pi/2} (1 - \gamma^2 \sin^2(y))^{-1/2} dy \ .$$

In the original variables, the period of a complete cycle of exchange of energy between the two harmonics is

$$L_\lambda = \frac{2K}{(v_c^2 - v_a^2)^{1/2} \alpha Q_1 (\alpha Q_2 E_0)^{1/2}} \ .$$

This distance will be called the repetition length of the system (the same parameter is named variously by other authors). This sort of periodic variation of the first two harmonics certainly accords qualitatively with what is observed in the laboratory (see again Figure 3(a)). An incoming wave train alluded to earlier that is especially interesting for our purposes is when $a_1^0 = 1/2$, $a_2^0 = 0$. The above formulae then simplify considerably:

$$r = v_a = x_a = 0,$$

$$v_b^2 = [1 + (\tfrac{\Delta Q}{4})^2]^{1/2} - \tfrac{\Delta Q}{4} \ , \quad v_c = \frac{1}{v_b} \ ,$$

$$\gamma = \frac{v_b}{v_c} = v_b^2 \ , \quad \tilde{L}_\lambda = 2 v_b K(v_b^2).$$

In the form just given, the system's predictions have been set against a considerable range of laboratory data (see Mei and Ünlüata, 1972). The results of this comparison show the repetition length, L_λ, to be rather well predicted, especially for larger values of ΔQ. since the repetition length seems to be a major factor as regards the spacing of bar-like structures in the bed, the reliability of the model in this aspect is welcome.

If the bed is spatially variable, an analytical solution is not available. However, for a given bottom configuration $h(x)$ it is an easy task to accurately approximate numerically the solution a_1 and a_2 of (1.21). The system of

equations is not stiff, and a straightforward application of the standard, fourth-order correct, Runge-Kutta discretization procedure gives very satisfactory results (cf. Isaacson and Keller, 1966). It is found that while the harmonic amplitudes $A_j(x) = |a_j(x)|$, $j = 1,2$, are not typically periodic over a gently-varying bed, they neverthless present a pattern of rhythmical exchange of energy. Examples of this phenomenon are pictured in Figure 6, where a fixed, incident

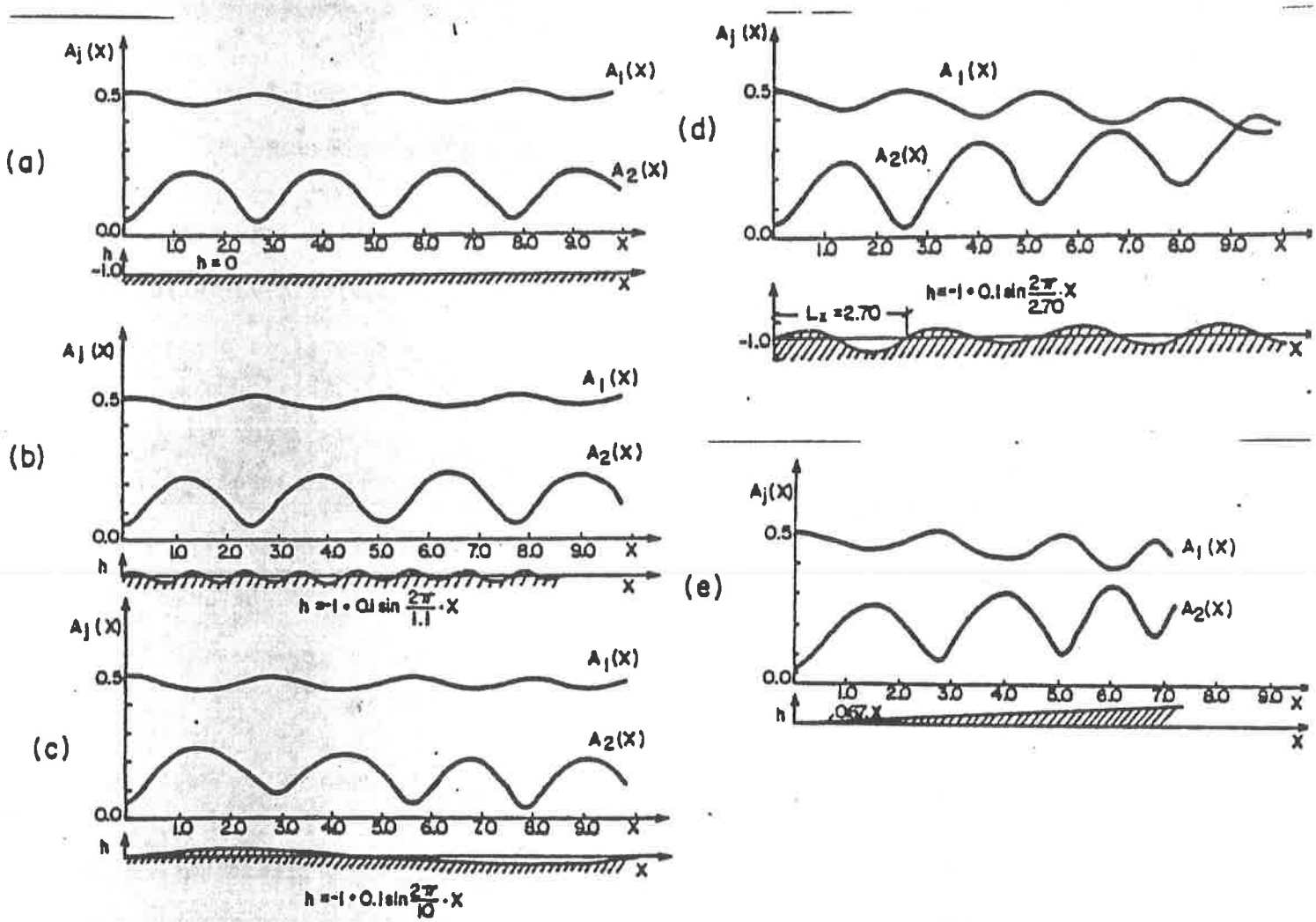

Figure 6. Rhythmical exchange of energy between the harmonic amplitudes $A_j(x) = |a_j(x)|$, $j = 1,2$, of an incident, sinusoidal wavetrain propagating over gently varying bed topographies: (a) a flat bed; (b) a wavy bed with corrugation-length scale shorter than the repetition length, L_λ; (c) a wavy bed with corrugation-length scale longer than the repetition length, L_λ; (d) wavy bed "tuned" to the repetition lenght, L_λ; (e) development of the wavetrain over a slightly sloped bed.

sinusoidal wavetrain is shown impinging on several, different slowly-varying bed topographies. Figure 6a shows the waves' response to a flat bed, and incidentally a nice display of the repetition that occurs over a flat bed. In 6b and 6c, the surface wave meets a wavy bed, but in both cases the length scale of the bed is quite different from the flat-bed repetition length. These bottom profiles draw about the same response as a flat bed. It is otherwise in 6d where the wavy bed is 'tuned' in length to the flat-bed repetition length, resulting in a substantial increase in the mean energy of the second harmonic. In 6e, an interesting example is presented where the wave encounters a gentle slope. Because the basic pattern of variation of A_1 and A_2 is similar over a wide range of topographies, it is tempting to use the term repetition length to mean the distance between successive minima of A_2, even in situations where this quantity varies with distance toward the shoreline. This terminology has proved to be of practical utility, and consequently it will be employed henceforth.

Turning now to equilibrium solutions, these are obtained from the full model by setting $\partial h/\partial T \equiv 0$ in (1.43), and solving the resulting system of equations. Since $\partial h/\partial T \equiv 0$, h is a function of x alone, and hence so are a_1 and a_2. Moreover, from (1.39), $\partial U_m/\partial x \equiv 0$, whence there is a constant Λ such that

$$U_m(x,T) \equiv \Lambda. \tag{2.8}$$

The constraint (2.8), when coupled with the Lau-Barcilon system (1.21), comprises the equations for a steady state, namely,

$$\begin{aligned} a_1'(x) + i\varepsilon f_1 f(x) a_1(x) + i\alpha Q_1 e^{i\Delta k x} a_1^*(x) a_2(x) &= 0, \\ a_2'(x) + i\varepsilon f_2 f(x) a_2(x) + i\alpha Q_2 e^{-i\Delta k x} a_1^{\,2}(x) &= 0, \end{aligned} \tag{2.9}$$

with

$$\sum_{j=1}^{2} \frac{\omega_j}{k_j} |a_j(x)|^2 [1 - \frac{\beta^2}{6} h^2(x) k_j^{\,2}]^2 D_j = \Lambda.$$

It is convenient in our analysis to write a_1 and a_2 in the form

$$a_j(x) = A_j(x) e^{i\phi_j(x)}, \tag{2.10}$$

for $j = 1,2$, where $A_j = |a_j|$ as before. Also let

$$\theta(x) = 2\phi_1(x) - \phi_2(x) - x\Delta k \ . \tag{2.11}$$

The existence of the conservation law (2.1) implies that the four real differential equations represented in complex form in (1.39) may be integrated once, as Armstrong et.al. (1962) have noticed. The resulting system is

$$\begin{aligned} \frac{dA_1}{dx} &= -\alpha Q_1 A_1 A_2 \sin(\theta), \\ \frac{dA_2}{dx} &= \alpha Q_2 A_1^2 \sin(\theta), \\ \frac{d\theta}{dx} &= -\Delta k - \varepsilon f(x)(2f_1 - f_2) + \alpha\left(Q_2 \frac{A_1^2}{A_2} - 2Q_1 A_2\right)\cos(\theta). \end{aligned} \tag{2.12}$$

The equations (2.12) are just the Lau-Barcilon equations in another guise. For steady configurations, they are still constrained by the last equation in (2.9),

$$\sum_{j=1}^{2} \frac{\omega_j}{k_j} A_j^2 \left[1 - \frac{\beta^2}{6} h^2(x) k_j^2\right]^2 D_j = \Lambda, \tag{2.13}$$

and the conservation law

$$\sum_{j=1}^{2} \frac{A_j^2}{Q_j} = \alpha E, \tag{2.14}$$

where E is a constant. Because of (2.13) and (2.14), A_1, A_2, θ, and h are not independent. For example, if A_1 is known, then A_2 is determined from (2.14), h is then obtained from (2.13), and θ is found using the last equation in (2.12). Thus in principle the system describing steady states may be further reduced to two equations in two unknowns, say A_2 and θ. All this is predicated upon knowledge of the various parameters in the problem, α, β, ω_i, k_i, Q_i, and f_i, for $i = 1,2$. These in turn are all determined once α and β are specified. (In the variables defined in (1.2), the fundamental wavelength is 1. Consequently $k_1 = 2\pi$ and ω_1, $\omega_2 = 2\omega_1$, and k_2 are determined by the dispersion relation, (1.11).) The amplitude and wavelength parameters, α and β respectively, can take any values consistent with the order of magnitude assump-

tions posited earlier. The values of E and Λ depend upon how a_1, a_2, and h have been normalized. If h_0 is taken to be the value of the initial depth at $x = 0$, then

$$h(0) = 1. \tag{2.15}$$

Moreover, because u and ζ are order-one quantities when referred to the variables as they appear here, it is natural to pose

$$A_1^2(0) + A_2^2(0) = \frac{1}{4} . \tag{2.16}$$

In addition the phase is normalized by the stipulation that

$$\theta(0) = 0 . \tag{2.17}$$

The simplest steady-state solutions are those where A_1, A_2, θ, and h are all x-independent, say equal to A_1^0, A_2^0, θ_0, and H_0, respectively. Such a solution necessarily satisfies

$$\begin{aligned} &\theta_0 = 0, \quad H_0 = 1, \quad f(x) \equiv 0, \\ &\Delta k - 2\alpha Q_1 A_2^0 + \alpha Q_2 \frac{(A_1^0)^2}{A_2^0} = 0, \end{aligned} \tag{2.18}$$

and

$$(A_1^0)^2 + A_2^0)^2 = \frac{1}{4} .$$

Combining the last two equations in (2.18) leads to a quadratic equation for A_2^0, say, from which one deduces immediately that

$$A_2^0 = \frac{-\Delta k + [(\Delta k)^2 + \alpha^2 Q_2(2Q_1 + Q_2)]^{1/2}}{2\alpha(2Q_1 + Q_2)} ,$$

$$A_1^0 = [\tfrac{1}{4} - (A_2^0)^2]^{1/2} ,$$

$$\theta_0 = 0, \qquad H_0 = 1. \tag{2.19}$$

The equilibrium configurations written in (2.19) are not especially interesting. In particular, the notion of a repetition length plainly has no validity in their regard. However, these solutions may be perturbed to produce time-independent

solutions with more structure.

To construct more general equilibrim configurations, it is helpful to reduce the system (2.12) along the lines already indicated. The choice of A_2 and θ as the primary dependent variables is convenient for the purposes at hand. Because of (2.14),

$$A_1^2(x) = Q_1[\alpha E - \frac{A_2^2(x)}{Q_2}], \tag{2.20}$$

and so A_1 is determined as the positive square root of the right-hand side of (2.20). For brevity, write

$$A_1(x) = F(A_2(x)), \tag{2.21}$$

where

$$F(y) = \{Q_1[\alpha E - \frac{y^2}{Q_2}]\}^{1/2}.$$

Using this relation in the last two equations in (2.12), there appear

$$\begin{aligned} \frac{dA_2}{dx} &= \alpha Q_2 F(A_2(x))^2 \sin\theta(x), \\ \frac{d\theta}{dx} &= -\Delta k + \varepsilon f(x)(f_2 - 2f_1) - 2\alpha Q_1 A_2(x)\cos\theta(x) \\ &\quad + \alpha[Q_2 \frac{F^2(A_2(x))}{A_2(x)}]\cos\theta(x). \end{aligned} \tag{2.22}$$

To complete the reduction to the two unknowns A_2 and θ, the depth variation $\varepsilon f(x) = h(x) - 1$ appearing in the second equation must be related to A_2 and θ. This is accomplished using (2.13) in conjunction with (2.21). Briefly, write

$$\begin{aligned} 0 = h^4(x) \sum_{j=1}^{2} \frac{\beta^4}{36} \omega_j k_j^3 A_j^2(x) D_j - h^2(x) \sum_{j=1}^{2} \frac{\beta^2}{3} \omega_j k_j A_j^2(x) D_j \\ + \sum_{j=1}^{2} \frac{\omega_j}{k_j} A_j^2(x) D_j - \Lambda \\ = Ah^4(x) - Bh^2(x) + C, \end{aligned} \tag{2.23}$$

say. Whenever A_1 appears, use (2.21) to express it in terms of A_2. The resulting quadratic equation may be solved thusly;

$$h^2(x) = \frac{B - [B^2 - 4AE]^{1/2}}{2A} = D,$$

say, so expressing h^2 as a function of A_2. The negative sign is taken in the solution of (2.23) because h is to be order one. Taking the positive square root, εf is obtained as a function of A_2,

$$\varepsilon f(x) = \frac{B - [B^2 - 4AE]^{1/2}}{2A} - 1 \qquad (2.24)$$

$$= G(A_2(x)).$$

Combining (2.24) with (2.22) gives a system for A_2 and θ, written symbolically as,

$$\frac{dA_2}{dx} = K(A_2, \theta),$$

$$\frac{d\theta}{dx} = L(A_2, \theta), \qquad (2.25)$$

where

$$K(y,z) = \alpha Q_2 F(y)^2 \sin(z)$$

and

$$L(y,z) = -\Delta k + (f_2 - 2f_1)G(y) - 2\alpha Q_1 y\cos(z) + \alpha[Q_2 \frac{F(y)^2}{y}]\cos(z).$$

The plane autonomous system (2.25) is investigated in a neighborhood of the constant solutions A_1^0, A_2^0, $\theta_0 = 0$, $H_0 = 1$ given in (2.18). The point (A_2^0, θ_0) comprises a critical point of (2.25), and therefore the behavior of the system close by this solution may be inferred from the properties of the linearized system

$$\frac{d(\delta A_2)}{dx} = \nabla K(A_2^0, \theta_0)\cdot(\delta A_2(x), \delta\theta(x)), \qquad (2.26)$$

$$\frac{d(\delta\theta)}{dx} = \nabla L(A_2^0, \theta_0)\cdot(\delta A_2(x), \delta\theta(x)),$$

near the origin (0,0). Here $\nabla K = (\partial K/\partial A_2, \partial K/\partial \theta)$ and similarly for ∇L. After a little manipulation, (2.26) is put into the simple form

$$\frac{d^2(\delta A_2)}{dx^2} = - \alpha Q_2 W_1 (A_1^0)^2 \delta A_2(x), \tag{2.27}$$

$$\frac{d\theta}{dx} = - W_1 \delta A_2(x),$$

where

$$W_0 = \frac{3A_1^0 \{\frac{\omega_2}{k_2}(1 - \frac{\beta^2}{6}k_2^2)^2 D_2 - \frac{\omega_1}{k_1}(1 - \frac{\beta^2}{6}k_1^2)^2 \frac{Q_1 D_1}{Q_2}\}}{\beta^2\{\omega_2 k_2(1 - \frac{\beta^2}{6}k_2^2)D_1(A_2^0)^2 + \omega_1 k_1(1 - \frac{\beta^2}{6}k_1^2)D_2(A_1^0)^2\}}$$

and

$$W_1 = W_0(2f_1 - f_2) + 4\alpha Q_1 + \alpha Q_2 \left(\frac{A_1^0}{A_2^0}\right)^2 .$$

As $W_1 > 0$ in the range of parameter values that interest us, the solutions of (2.27) are periodic of period $2\pi/(A_1^0\sqrt{\alpha Q_2 W_1})$. Thus infinitesimal perturbations of the constant states show periodicity, a kind of infinitesimal version of the repetition length discussed earlier, only now the bottom also has a periodic structure.

In any case, the foregoing calculations imply that (0,0) is a center for the linearized system (2.26), and the general theory of plane autonomous systems (cf. Coddington and Levinson, 1955, chapter 15) assures that (A_2^0, θ_0) is itself a center, or else a spiral point, of the full nonlinear system (2.25).

The possibility of (A_2^0, θ_0) being a spiral point is discarded using the following argument. Supposing the contrary, let $(A_2(x), \theta(x))$ be an orbit of (2.25) that spirals into the critical point $(A_2^0, \theta_0) = (A_2^0, 0)$, say as $x \to +\infty$. Then by a translation of the independent variable, the normalization (2.17) that $\theta(0) = 0$ may be enforced. Let $\alpha > 0$ be the first zero of $\theta(x)$ for $x > 0$. Such a point a exists since $(A_2(x), \theta(x))$ spirals around $(A_2^0, 0)$. Define new functions $(r(x), \phi(x))$ on $[-a,a]$ as follows:

$$r(x) = \begin{cases} A_2(x), & 0 \le x \le a, \\ A_2(-x), & -a \le x \le 0, \end{cases} \qquad \phi(x) = \begin{cases} \theta(x), & 0 \le x \le A, \\ -\theta(-x), & -a \le x \le 0. \end{cases} \tag{2.28}$$

A close examination convinces one that $(r(x),\phi(x))$ is a solution of (2.25) on the entire interval of its definition, and that $(r(a),\phi(a)) = (r(-a),\phi(-a))$. Extending the functions (r,ϕ) to all x by asking that they be periodic of period $2a$, we obtain a closed orbit, that is, a periodic solution of (2.25). It follows that $(r(x),\phi(x)) = (A_2(x),\theta(x))$ for all x, since if two orbits intersect they are identical, by uniqueness of solutions to the initial-value problem. This contradicts the assumption that (A_2,θ) spirals in to $(A_2^0,0)$ and proves that (A_2^0, θ_0) is a center.

Figure 7 shows the dependence of the infinitesimal repetition length, the periods of the solutions of the linearized system (2.26), as a function of α and β. Note that L_λ decreases with an increase in either α or β, but that L_λ depends more strongly on β than on α. This squares with the trends observed in the laboratory for the repetition length over a horizontal bed (see Figure 8).

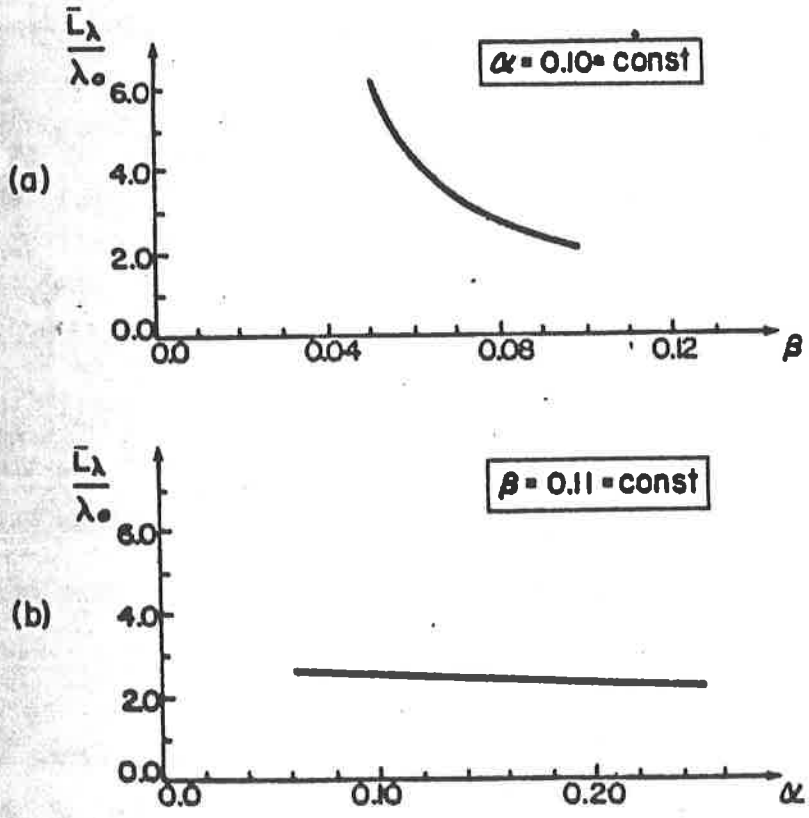

Figure 7. Dependence of the infinitesimal repetition length, L_λ, the periods of the solution of the system (2.24), as a function of the wave parameters

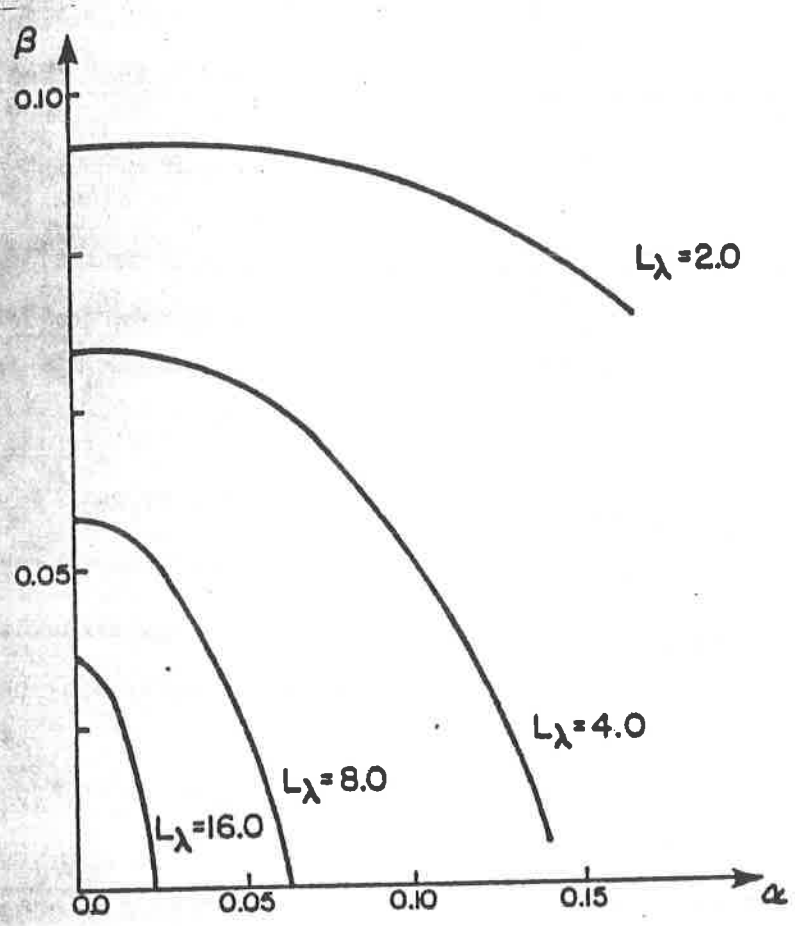

Figure 8. Wavetank data for the repetition length $\overline{L}_\lambda/\lambda_0$ as a function of the wave parameters: (a) β with α = const, (b) α with β = const; (after Boczar-Karakiewicz and Bona, 1981).

The presence of periodic solutions to the linearized system is taken as an encouraging outcome, suggesting that it would be worthwhile to study the full, time-dependent version of the model. In this respect, the steady configurations can play another useful role, serving as 'exact' solutions on which to test the accuracy of a time-dependent numerical scheme. These developments are reported in the next Section.

3. Time-Dependent Configurations

The qualitative match of theory and experiment obtained in Section 2 regarding the steady-state solutions of the model suggested that the investigation of time-dependent solutions was worthwhile. In this section, a series of numerical integrations of the complete, time-dependent set of equations (1.43) will be

described. In the present paper, only two types of initial bottom profiles are examined, namely, a ramp configuration (used in the wavetank experiments of Boczar-Karakiewicz et al. 1981, see Figure 1) and a flat bottom. In later stages of this investigation, more complex initial bed profiles will be introduced. Of especial interest are gently sloping beds which are typical of many different field situations.

A standard, forth-order correct, Runge-Kutta algorithm was used to integrate the first two equations in (1.43). A predictor-corrector scheme with a small amount of artificial damping was used to advance the bottom to the next time level. More precisely, the strong evidence of two, very disparate time scales, as described in Section 1, indicated that it would be propitious to decouple the temporal and spatial integrations. At a fixed time T, the wave harmonics the bed configuration $h(x,T)$ to be fixed. The updated bedform $h(x,T+\Delta T)$ is then determined from the third equation in (1.43). The process is then iterated. It gets its start from the given initial bed profile, of course.

The precise technique utilized is now described. The region of space and time of interest is the rectangle comprised of those points (x,T) for which $0 < x < M$ and $0 < T < T_0$. Consider the grid $(i\Delta x, j\Delta T)$ in (x,T) space where i and j are integers with $0 < i < N$, $0 < j < J$, $M = N\Delta x$, and $T_0 = J\Delta T$. For $x = i\Delta x$ and $T = j\Delta T$, let h^{ij} denote the approximate value of $h(x,T)$, and let f^{ij} denote the approximate value of $f(x,T)$, where f is the function defined in (1.8) that corresponds to h. Let a_1^{ij} and a_2^{ij} denote the approximate values of a_1 and a_2, respectively, at the same spatial and temporal point. Suppose at time T that h^{ij} is known for each value of i between 0 and N. Then values of a_1^{ij} and a_2^{ij}, for $0 < i < N$, are computed from equation (1.21) using the standard, forth-order correct, Runge-Kutta scheme (cf. Isaacson & Keller, 1966, Ch. 8). The boundary conditions explained in (1.19) are imposed in the form

$$a_1^{0j} = a_1^0 \quad \text{and} \quad a_2^{0j} = a_2^0 ,$$

and used to initiate the numerical integration of (1.21). Once a_1^{ij}, a_2^{ij}, and h^{ij}, $0 \leq i \leq N$, are in hand, an approximation ϕ^{ij} to the function U_m at the points $x = i\Delta x$, $0 \leq i \leq N$, at time T is immediately available by application of formulas (1.40) and (1.41). A fourth-order approximation y^{ij} to $\partial U_m/\partial x$ at the points $x = i\Delta x$, $T = j\Delta T$, $0 \leq i \leq N$, is then obtained using standard, centered difference formulas, with appropriate modifications near the left- and right-hand endpoints of the spatial domain. An updated approximation $h^{i,j+1}$, $0 \leq i \leq N$, of the bottom profile is then obtained using a split-step technique consisting of the fourth-order correct Moulton's method (see, again, Isaacson & Keller, 1966) to predict a first version $\tilde{h}^{i,j+1}$ of the bottom followed by an averaging step

$$h^{i,j+1} = [\tilde{h}^{i-1,j+1} + \tilde{h}^{i,j+1} + \tilde{h}^{i+1,j+1}]/3.$$

The initial bottom profile, $h(x,0)$, is used to start Moulton predictor step for the case $j = 0$.

The spatial averaging that is featured in the method outlined above is used to add stability to the computational algorithm. It amounts to integrating the nonlinear parabolic equation

$$\frac{\partial h}{\partial T} = \frac{\gamma \Delta x}{3} \frac{\partial^2 h}{\partial x^2} + \frac{\partial \phi}{\partial x} \quad \text{where} \quad \gamma = \lim_{\substack{\Delta x \to 0 \\ \Delta T \to 0}} \frac{\Delta x}{\Delta T} > 0. \tag{3.1}$$

rather than the conservation law

$$\frac{\partial h}{\partial T} = \frac{\partial \phi}{\partial x}. \tag{3.2}$$

The damping term deserves some comment. As far as the present article is concerned, this term is strictly artificial, and has been introduced to stabilize the temporal integration. However, we will argue in subsequent studies that a term something like this should appear when more detailed modelling of the sedimentation process is considered. As long as the solution of the differential equation (3.2) is smooth, then the error introduced by the damping term becomes negligible in the limit as the discretization parameters Δx and ΔT tend to zero appropriately.

The reliability of the integrations was checked in some detail. The temporal integration gave more trouble and the solutions did vary slightly (a maximum of about 10%) as ΔT was decreased, but their global behavior did not change significantly. As regards the spatial integration, a convergence study was performed with decreasing values of Δx. For such a study the exact, constant solutions of the steady-state equations (2.19) were used as test cases. For these solutions, the values of ζ_1 and ζ_2 must vary by quantities that are of order one so that A_1 and A_2 remain constant. Figure 9 shows a log-log plot of the absolute value of the maximum error in A_1 and A_2 over the spatial interval (0,10). The ordinate gives the percentage error and the abscissa shows the number of intervals used in the spatial integration. Notice that at a point lying between $\Delta x = 1/16$ and $\Delta x = 1/32$ numerical roundoff appears to prohibit any further increase in the accuracy of the integration. The slope of the dotted line shows how accuracy should behave in the fourth order scheme. This behavior is observed in the range where $\Delta x > 1/16$.

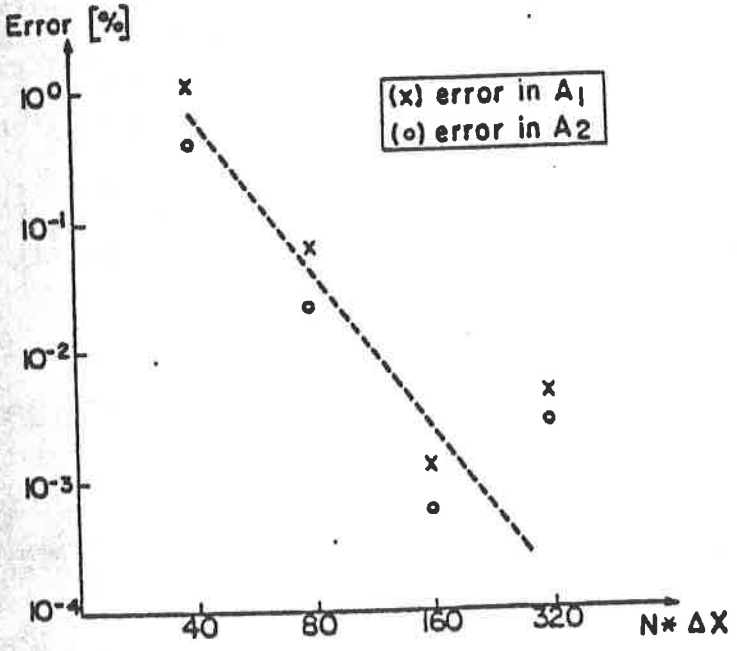

Figure 9. A convergence study of the numerical scheme for integrating the model equations (2.19). The predicted convergence rate for the integration algorithm used should be $O(\Delta x^4)$.

Figure 10 depicts several stages of the evolution of an initial ramp bottom profile as well as the associated wave field's harmonic components. The incident

wave field is characterized by $\alpha = 0.1$ and $\beta = 0.08$, values that correspond closely to values of these parameters that obtain in actual flume experiments. The depth changes relatively rapidly in the earlier stages of the integration, but the entire system settles down to an equilibrium configuration in due course (shown at $T = 640\Delta T$). Notice in Figure 10 that the left-hand side of the (x,ζ) domain, where the waves enter the system, appears to reach its final configuration first. This corresponds to what is observed in wavetank experiments (see again Figure 1 and the article of Boczar-Karakiewicz et al. 1981).

A sample of the long term equilibrium solutions of our model system is presented in Figure 11. In these examples, the bottom configuration was completely flat at $T = 0$, and incident wave field was given four different pairs of parameter values ($\alpha = 0.05$ and 0.15, $\beta = 0.07$ and 0.09). Notice that the equilibrium repetition lengths appearing in Figure 11 vary with α and β in the same way that they do in the graph in Figure 7. The repetition length decreases with increasing α and β, and depends much more strongly upon β than α.

The equilibrium states of Figures 10 and 11 are all qualitatively similar. In more extensive studies we have found that a comparatively wide range of initial bottom configurations evolves into equilibrium bottom configurations that are periodic in x with a well defined repetition length that characterizes both the exchange of energy between the first and second harmonic components and the bottom variation. Again, this is the same state of affairs that obtains in wavetank experiments.

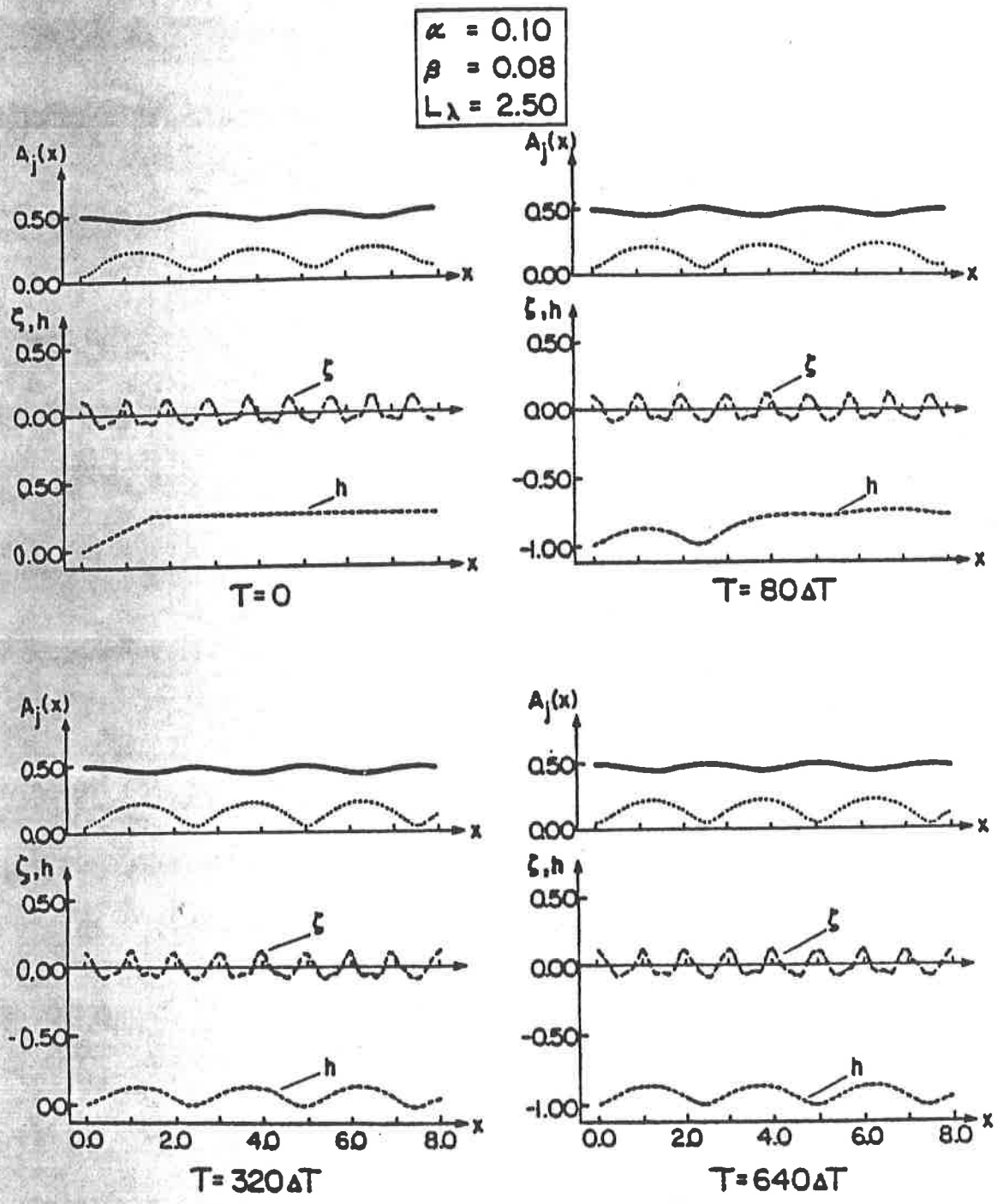

Figure 10. Final state solution (at $T = 640\Delta T$) of the time dependent model equations starting at $T = 0$ from an initial ramp bottom profile. The horizontal coordinate gives distances in units of the wavelength, the incident wave parameters are $\alpha = 0.10$ and $\beta = 0.08$; - connotes the value of $A_1(x)$ and --- connotes the value of $A_2(x)$.

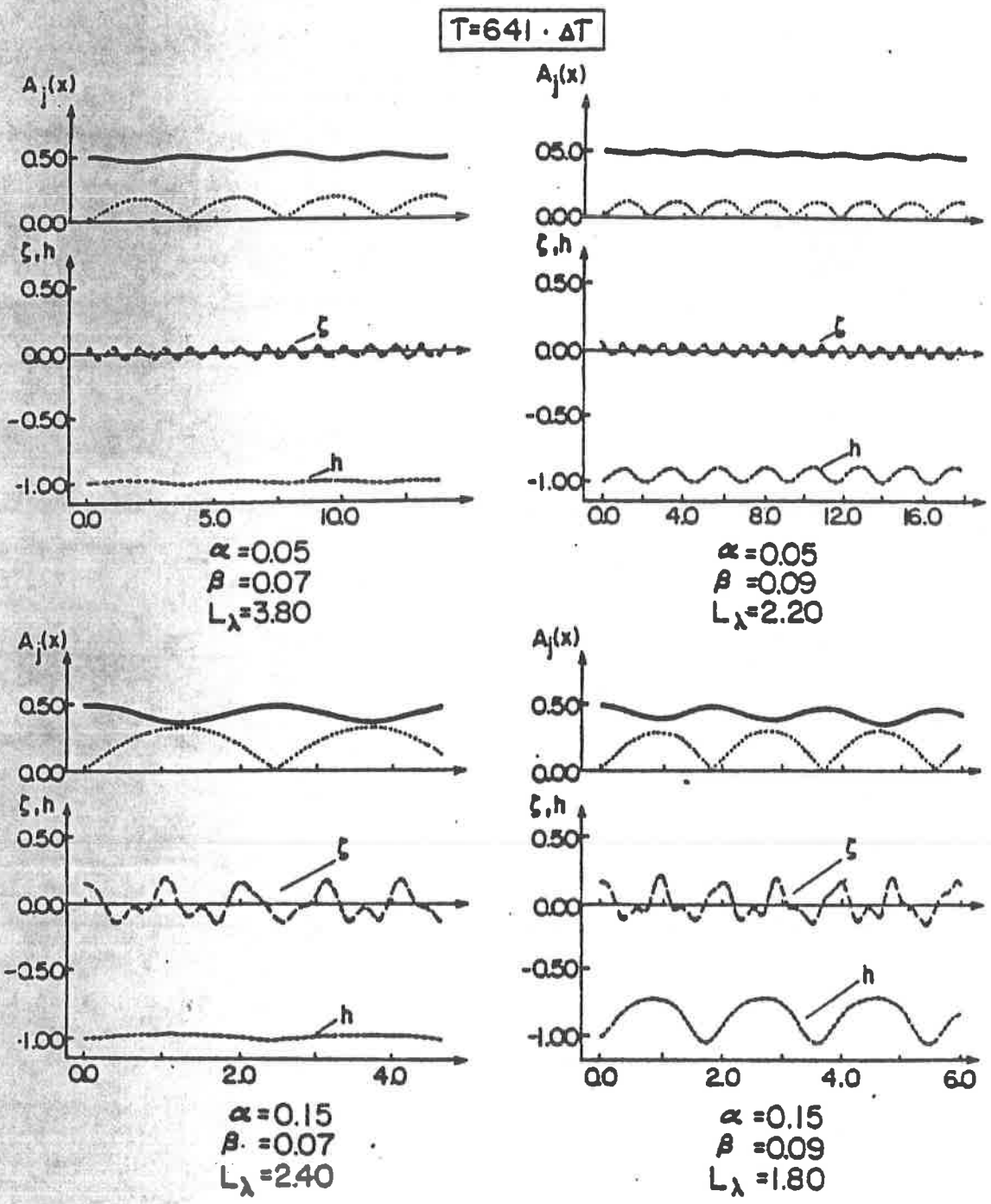

Figure 11. Final state solution (at $T = 641\Delta T$) of the time dependent model equations starting at $T = 0$ from an initial flat bottom profile. The horizontal coordinate gives distances in units of the wavelength, the incident wave parameters are $\alpha = 0.05$ and 0.015; $\beta = 0.07$ and 0.09; L_λ denotes the corresponding repetition length; - connotes the values of $A_1(x)$ and --- connotes the values of $A_2(x)$.

4. Conclusions

It is a well known fact that the interaction of shallow water waves and bottom sediment may lead to the formation of equilibrium bar and trough configurations. Here we have used a simple, two-dimensional model to relate the change over time of a bottom profile to the spatial development of the wavefield's first and second harmonics. The resulting set of equations has been investigated both for equilibrium solutions and for time-dependent solutions. It has been found that time-dependent solutions may evolve toward an attractor which is an equilibrium solution.

Although data from wavetank experiments does not yet permit realistic quantitative comparison with our theory, the length scales and qualitative features predicted by our model agree tolerably well with laboratory findings. Preliminary experience with the model as regards field situations also holds up promise for its utility (cf. Boczar-Karakiewicz and Bona 1981, Boczar-Karakiewicz et al. 1984). Further investigation of the model's predictive power in both laboratoy and especially field situations seems warranted.

It is worth emphasis that the model developed here has been kept as simple as possible, and that there are many ways in which it might be improved. First, reflection is important on many real beaches, and this should certainly be taken into account in modelling the wave field. Secondly, dissipation of the wave field is important in some regimes to which the model might apply, and this too should be incorporated into the model. At a more sophisticated level, there is no reason why Boussinesq or Korteweg-de Vries type equations could not be used in modelling the wavefield, rather than passing to the two-harmonic approximation. One could even imagine retaining the full Euler equations if need be. More complex models for the boundary layer and the associated mass transport could be incorporated (cf. Bagnold 1963, Drew 1979, or Bowen 1980). And, one need not fix the sediment distribution in the fluid, but rather determine this locally according to the wave field. Finally, it would be worthwhile extending the model in the other spatial dimension, so allowing for some gradual variation along a coastline.

We expect to report on various of these theoretical and practical issues at a later stage.

References

Abbott, M.B. 1960. Boundary layer effects in estuaries. J. Mar. Res., 18: 83-100.

Amick, C.J. 1984. Regularity and uniqueness of solutions of the Boussinesq systems of equations. J. of Diff. Equ., 54: 231-247.

Armstrong, J.A., N. Bloombergen, J. Ducuing and P.S. Pershan. 1962. Interaction between light waves in a nonlinear dielectric. Phys. Rev., 127: 168-177.

Bagnold, R.A. 1963. Mechanics of marine sedimentation. In: The Sea, Hill, M.N. (ed.) Wiley-Interscience, New York, 3: 507-528.

Benjamin, T.B., B. Boczar-Karakiewicz and W.G. Pritchard. (To appear). Formation of sand bars by waves. Part 1: Flow over fixed beds.

Benjamin, T.B., J.L. Bona and J.J. Mahony. 1972. Model equations for long waves in nonlinear dispersive systems. Phil. Trans. Roy. Soc. Lond., Series A, 272: 47-78.

Boczar-Karakiewicz, B., B. Paplinska and J. Winiecki. 1981. Formation of sand bars by surface waves in shallow water. Laboratory experiments. Rozprawy Hydrotechniczne, 43: 111-125.

Boczar-Karakiewicz, B. and J.L. Bona. 1981. Uber die riffbildung an sandigen küsten durch progressive wellen. Mitteilungen des Leichtweiß-Instituts für Wasserbau der Technischen Universität Braunschweig, 70: 380-420.

Boczar-Karakiewicz, B., G. Drapeau and B.F. Long. 1984. Modélisation des barres sableuses littorales de la partie nord des Iles-de-la-Madeleine. Sciences et Techniques de l'Eau, 17: 35-39.

Bona, J.L., W.G. Pritchard and L.R. Scott. 1981. An evaluation of a model equation for water waves. Phil. Trans. Roy. Soc. Lond., Series A, 302: 457-510.

Bona, J.L. and V.A. Dougalis. 1980. An initial- and boundary-value problem for a model equation for propagation of long waves. J. Math. Anal. Appl., 75: 501-522.

Bona, J.L. and R. Smith. 1976. A model for the two-way propagation of water waves in a channel. Math. Proc. Camb. Phil. Soc., 79: 167-182.

Boussinesq, J. 1871. Théorie de l'intumescence liquide appelée onde solitaire ou de translation se propageant dans un canal rectangulaire. Comptes Rendus, 72: 755-759.

Bowen, A.J. 1980. Simple models of nearshore sedimentation; beach profiles and longshore bars. In: The Coastline of Canada, McCann, S.B. (ed.), Geological Survey of Canada, paper 80-10: 1-11.

Bowen, A.J. and D.L. Inman. 1971. Edge waves and crescentic bars. J. Geophys. Res., 76: 8662-8671.

Carter, T.G., P.L.F. Liu and C.C. Mei. 1973. Mass transport by waves and offshore sand bedforms. J. Waterways, Harbours, Coastal Eng., 99: 165-184.

Coddington, E.A. and N. Levinson. 1955. Theory of ordinary differential equations. McGraw-Hill, New York.

Drew, D.A. 1979. Dynamic model for channel bed erosion. J. Hydraulics Division A.S.C.E., 105: 721-735.

Druet, Cz, S.R. Massel, and R. Zeidler. 1972. The structure of wind waves in the southern coastal zone of the Baltic Sea. Rozprawy Hydrotechniczne, 30: 312-318 (in Polish).

Elgar, S. and R.T. Guza. 1985. Shoaling gravity waves: comparison between field observations, linear theory and a nonlinear model. J. Fluid Mech., 158: 47-70.

Greenwood, B. and R.G.D. Davidson-Arnott. 1979. Sedimentation and equilibrium in wave-formed bars: A review and case study. Can. J. Earth Sci., 16: 312-332.

Hammack, J.L. 1973. A note on tsunamis: their generation and propagation in an ocean of uniform depth. J. Fluid Mech., 60: 769-799.

Hammack, J.L. and H. Segur. 1974. The Korteweg-de Vries equation and water waves. Part 2. Comparison with experiments. J. Fluid Mech., 65; 289-314.

Isaacson, E. and H.B. Keller. 1966. Analysis of numerical methods. John Wiley, New York.

Johns, B. 1970. On the mass transport induced by oscillatory flow in a turbulent boundary layer. J. Fluid Mech., 43: 177-185.

Johns, B. 1975. The form of the velocity profile in a turbulent shear wave boundary layer. J.Geophys. Res., 80: 5109-5112.

Johns, B. 1977. Residual flow and boundary shear stress in the turbulent bottom layer beneath waves. J. Phys. Oceanogr. 7: 733-738.

Johnson, R.S. 1973. On the development of a solitary wave moving over an uneven bottom. Proc. Camb. Phil. Soc., 73: 183-203.

Kakutani, T. 1971. Effect of an uneven bottom on gravity waves. J. Phys. Soc. Japan, 30: 272-276.

Kortweg, D.J. and G. de Vries. 1895. On the change of form of long waves advancing in a rectangular channel, and on a new type of long stationary waves. Phil. Mag., 5: 422-443.

Lau, J. and A. Barcilon. 1972. Harmonic generation of shallow water waves over topography. J. Phys. Oceanogr., 2: 405-410.

Lau, J. and B. Travis. 1973. Slowly varying Stokes waves and submarine longshore bars. J. Geophys. Res., 78: 4489-4497.

Longuet-Higgens, M.S. 1953. Mass transport in water waves. Phil. Trans. Roy. Soc. Lond., Series A, 245: 535-581.

Longuet-Higgens, M.S. 1981. Oscillating flow over steep sand ripples. J. Fluid Mech., 107: 1-35.

Madsen, O.S. 1971. On the generation of long waves. J. Geophys. Res., 76: 8672-8683.

Madsen, O.S. and C.C. Mei. 1969. The transformation of a solitary wave over an uneven bottom. J. Fluid Mech., 39: 781-791.

McClain, C.R., N.E. Huang and L.J. Pietrafesa, 1977. Application of a radiation type boundary condition to the wave, porous bed problem. J. Phys. Oceanogr., 7: 823-835.

Mei, C.C. and B.L. Mehauté. 1966. Note on the equations of long water waves over an uneven bottom. J. Geophys. Res., 71: 393-400.

Mei, C.C. and U. Ünlüata. 1972. Harmonic generation of shallow waves. In: Waves on beaches and resulting sediment transport, Meyer, R.E., (ed.), Academic Press, New York: 181-202.

Peregrine, D.H. 1972. Equations for water waves and the approximation behind them. In: Waves on beaches and resulting sediment transport, Meyer, R.E. (ed.), Academic Press, New York: 95-121.

Peregrine, D.H. 1967. Long waves on a beach. J. Fluid Mech., 27: 815-825.

Raudkivi, A.J. 1976. Loose boundary hydraulics. 2nd edition, Pergamon Press, Oxford.

Russel, R.C.H. and J.D.C. Osorio. 1958. An experimental investigation of drift profiles in a closed channel. Proc. 6th Conf. Coast. Eng., London: 171-193.

Schonbek, M.E. 1981. Existence of solutions for the Boussinesq system of equations, J. Diff. Equa., 52: 325-352.

Sleath, J.F.A. Measurements of bed load in oscillatory flow. J. Waterway Port Coast. Ocean Div., 4: 291-322.

Stokes, G.G. 1847. On the theory of oscillatory waves. Trans. Camb. Phil. Soc. Collected papers, 1: 197-229.

Svendsen, I.A. and J. Buhr-Hanson. 1978. On the deformation of periodic long waves over a gently sloping bottom. J. Fluid Mech., 87: 433-448.

Thornton, E.B., J.J. Galvin, F.L. Bub and D.P. Richardson. 1976. Kinematics of breaking waves. Proc. 15th Conf. Coast. Eng., Honolulu: 460-476.

Thornton, E.B. and G. Schaeffer. 1978. Probability density functions of breaking waves. Proc. 16th Conf. Coast. Eng., Hamburg: 507-519.

Van de Graff, I. and W.M.K. Tilmans. 1980. Sand transport by waves. Proc. 17th Coast. Eng. Conf., Sydney: 1140-1157.

Whitham, G.B. 1974. Linear and nonlinear waves. John Wiley & Sons, New York.

Winther, R. 1982. Finite element method for a version of the Boussineq equation. SIAM J. Num. Anal., 19: 561-570.

Zabusky, N.J. and C.J. Galvin. 1971. Shallow-water waves, the Korteweg-de Vries equation and solitons. J. Fluid Mech., 47: 811-824.

Zenkovitch, V.P. 1967. Processes of coastal development. Interscience, New York.

PSU APPLIED MATHEMATICS REPORT SERIES

AM 1: BENJAMIN, T.B., BOCZAR-KARAKIEWICZ, B. & PRITCHARD, W.G. Oct. 1986 Reflection of water waves in a channel with corrugated bed.

AM 2: ALBERT, J.P., BONA, J.L. & HENRY, D.B. Oct. 1986 Sufficient conditions for stability of solitary solutions of model equations for long waves.